TABLE 7. UNIT-CELL CONTENTS FOR AN AMPHIBOLE OF BINNS (1965), CALCULATED USING THE METHOD OF ESTIMATING THE MINIMUM AND MAXIMUM BOUNDS OF THE Fe^{2+} AND Fe^{3+} CONTENTS

Analysis			Min.	Max.	23(O)	24(O,OH,F)
SiO_2	40.85	Si	6.28	6.18	6.20	6.25
Al_2O_3	14.45	Al	1.72	1.82	1.80	1.75
TiO_2	0.65	ΣT	8.00	8.00	8.00	8.00
Fe_2O_3	5.59					
FeO	18.53	Al	0.89	0.75	0.79	0.86
MnO	0.35	Ti	0.08	0.07	0.07	0.08
MgO	5.11	Fe^{3+}	0.12	0.86	0.64	0.64
CaO	10.86	Fe^{2+}	2.91	2.12	2.35	2.37
Na_2O	1.48	Mn	0.05	0.05	0.05	0.05
K_2O	0.61	Mg	1.17	1.15	1.16	1.17
H_2O	1.62	ΣC	5.21	5.00	5.06	5.16
F	0.00					
		ΣC-5	0.21	-	0.06	0.16
		Ca	1.79	1.76	1.77	1.78
		Na	-	0.24	0.17	0.06
		ΣB	2.00	2.00	2.00	2.00
		Na	0.44	0.19	0.26	0.38
		K	0.12	0.12	0.12	0.12
		ΣA	0.56	0.31	0.38	0.50

balance equation, $Fe^{3+} = {}^{iv}Al + Na^{M(4)} - (Na,K)^{A} - {}^{vi}Al - 2Ti^{4+}$, repeated the normalization procedure and calculated a new Fe^{3+} content, iterating this procedure until there was no change in the derived Fe^{+3}/Fe^{2+} ratio. An example is given in Table 7. It has been suggested that the halfway point between minimum and maximum Fe^{3+} contents be taken as an estimate of the actual Fe^{3+} content. This premise was tested for calcic and subcalcic amphiboles on the superior analyses from the compilation of Leake (1968); the results are shown in Figure 7, where it can be seen that there is (unfortunately) no significant correlation between the observed and calculated values. This is really not surprising if we consider the constraints used in the calculations; the actual values of the bounds will be functions of such factors as the amount of Fe–Mn–Mg amphibole substitution in calcic amphibole and the amount of alkali amphibole substitution in calcic amphibole, factors that are a function of bulk-rock chemistry and environment. Perhaps a detailed correlation between these calculations and the specific paragenesis of each amphibole could lead to a better estimate. It is implicit in these methods that the formula unit contains 2(OH,F,Cl); deviation from this condition will further affect the Fe^{3+}/Fe^{2+} ratios and calculations of the unit-cell content.

The Amphibole Crystal Structures

The basic amphibole structure was first characterized by Warren (1929) when he solved the crystal structure of tremolite. Evidence of structural unity throughout the minerals of the amphibole group was provided by Warren (1930) in a general survey of the structure and chemistry of the monoclinic amphiboles, and by Warren & Modell (1930b) in their solution to the crystal structure of anthophyllite. Tschermak (1872) had recognized that there was a strong relationship between the chemistry, physical properties and paragenesis of the pyroxenes and the amphiboles. Warren (1929) and Warren & Modell (1930b) showed that this relationship also extended to the unit-cell dimensions (Fig. 8) and diffraction patterns, and used this relationship to solve the structures of tremolite and anthophyllite by analogy with the known structures of diopside (Warren & Bragg 1928) and enstatite (Warren & Modell 1930a). Warren (1930) noted the striking similarity of the *h0l* reflections in tremolite and diopside, and, coupled with the similarity of the unit-cell dimensions in this projection, concluded that on the (010) projection, the tremolite and diopside structures were practically identical. Thus, the tremolite structure was constructed by incorporation within the tremolite unit-cell of "blocks of the diopside structure" and "reflexion planes". Warren found that there were only two possible relative positions of the "diopside blocks" and the mirror planes that generated a reasonable structural arrangement; as only one of these arrangements was commensurate with the measured *b* parameter of the tremolite unit-cell, the essential features of the tremolite structure were determined. The remaining atoms (2 Mg) were located by symmetry and bond-valence arguments, as were the presence and position of the hydroxyl group in the structure. Structure-factor calculations confirmed the derived atomic arrangement.

The essential feature of the amphibole structure (Fig. 11) is a double chain of corner-linked tetrahedra that extends infinitely in one direction and has the general stoichiometry $(T_4O_{11})_\infty$. The direction of infinite polymerization of the double-chain unit defines the *Z* axis of the amphibole cell in the normal orientation. The actual value of the repeat distance in the *Z*

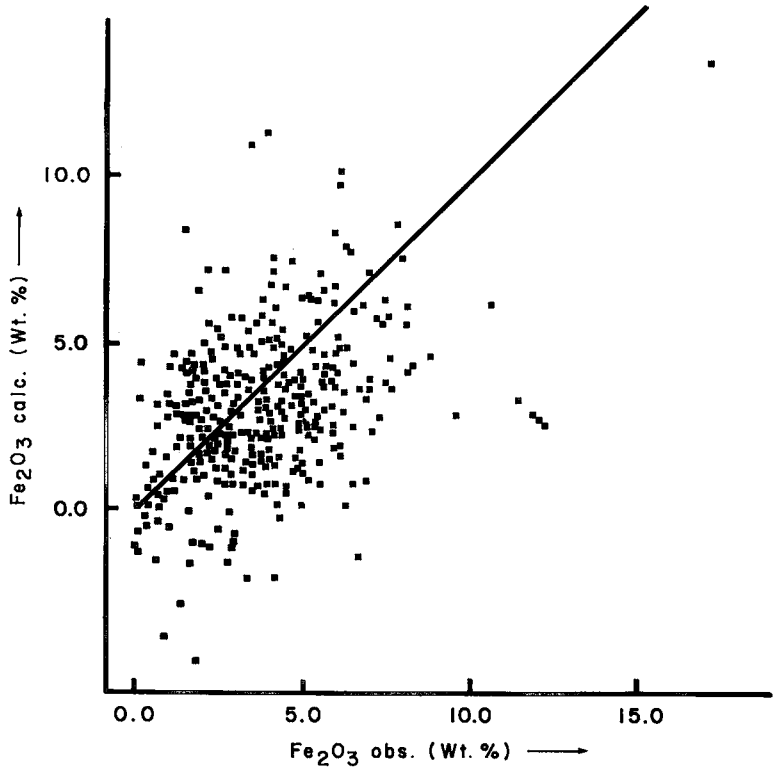

FIG. 7. Fe^{3+} p.f.u. calculated by the method of Papike *et al.* (1974) compared with the observed value [based on a 24(O, OH, F) calculation] for the superior analyses of Leake (1968).

direction is the *c* dimension of the unit cell and is dependent on such factors as the type of tetrahedrally co-ordinated cation and the stereochemistry of the tetrahedra; however, these factors produce only minor perturbations from the ideal value of ~5.3 Å for an $(Si_4O_{11})_\infty$ chain. It is convenient to recognize two different types of oxygen anions in this double-chain element. The oxygen atoms lie approximately in two planes parallel to the chain direction; all oxygen atoms lying in the plane containing the linkages between adjacent tetrahedra are called basal oxygen, whereas the oxygen atoms lying in the other plane are called apical oxygen. Oxygen atoms bonded to two tetrahedrally co-ordinated cations are called bridging (linking two TO_4 tetrahedra together) and here are denoted as O(br), whereas oxygen atoms bonded to one tetrahedrally co-ordinated cation are called nonbridging and here are denoted as O(nbr).

The $(T_4O_{11})_\infty$ chains are linked together by intermediate-size (0.53–0.83 Å) divalent and trivalent cations that bond to the O(nbr) anions of the chains. Two types of interchain linkage may be recognized. A strip of these divalent and trivalent cations is intercalated between two layers of apical oxygen atoms belonging to double chains that adjoin each other orthogonal to the plane of the basal oxygen atoms. The adjacent double-chains are staggered in the *Z* direction so that the apical oxygen atoms of adjacent chains assume a pseudo-octahedral arrangement around each of the linking divalent and trivalent cations. In order to complete the co-ordination of the cations in the centre of this strip, it is necessary to add another anion to the plane of the apical oxygen atoms; this is the monovalent anion in the amphibole formula. Thus these adjacent double-chains are tightly bonded together and form a modular unit (an I-beam) that plays an important role in the model structures that will be described later. The second type of interchain linkage joins these modular units together in a three-dimensional array (Fig. 9). The divalent and

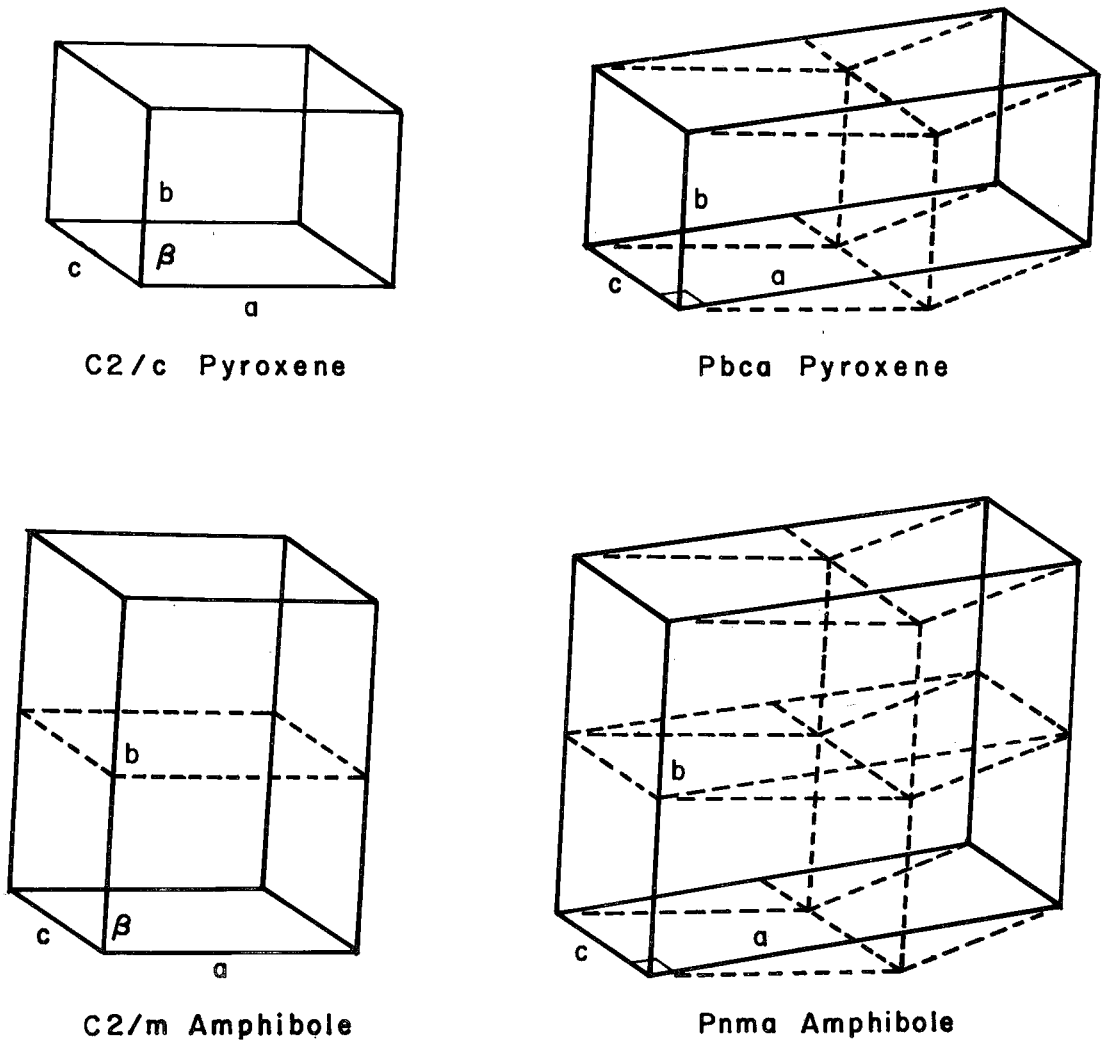

FIG. 8. The relationship between the cells of the pyroxenes and the amphiboles [after Warren & Modell (1930b)].

trivalent cations at the edges of the I-beam unit link laterally to the nonbridging basal oxygen atoms of adjacent I-beams. These divalent and trivalent cations, together with their co-ordinating anions, define a strip of edge-sharing octahedra that extends infinitely in the *Z* direction. Thus, an I-beam may also be thought of as a strip of edge-sharing octahedra sandwiched between two double-chains of corner-sharing tetrahedra.

As described thus far, the structure consists of C- and T-type cations. Further linkage between the modular units is provided by the A and B cations. The B cations are situated at the margins of the octahedral strips, where they provide additional linkage both within individual I-beams and between adjacent I-beams. The interchain linkage provided by the B-type cations differs from the second type of interchain linkage described above. The C-type cations all bond to nonbridging anions whereas the B-type cations bond both to nonbridging and bridging anions. The B cations are surrounded by eight anions, not all of which are necessarily bonded to the central cation; these anions are arranged in a

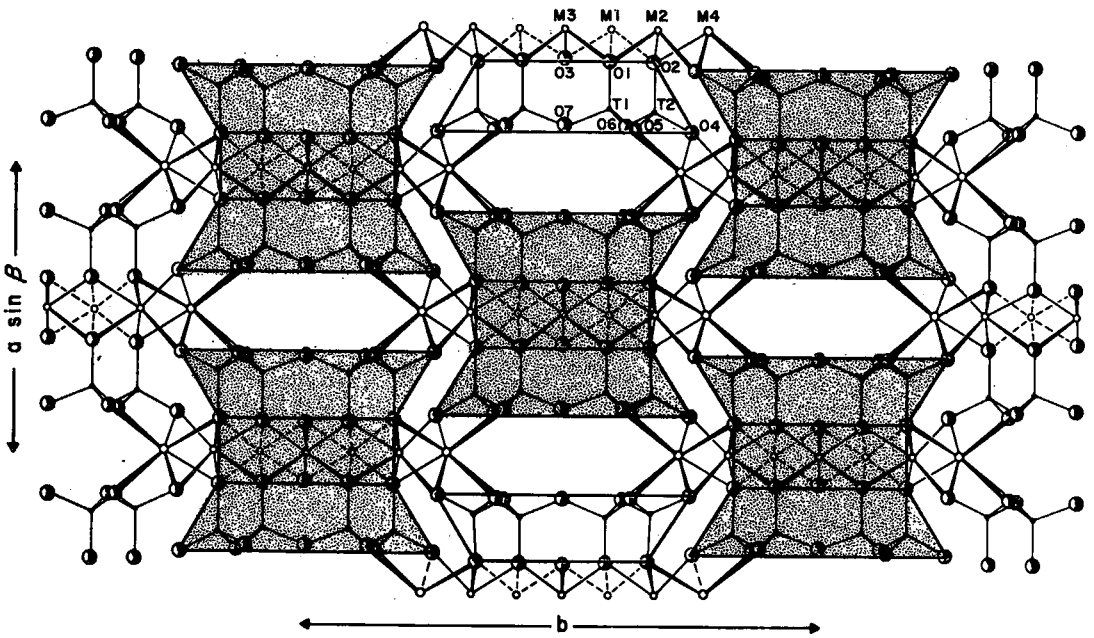

FIG. 9. The crystal structure of $C2/m$ amphibole projected down Z; the shaded areas show the I-beam modules of the structure [after Cameron & Papike (1979)].

distorted square antiprism, the exact configuration of which is a function of the central cation and local structural requirements. Between the back-to-back double-chains is a large cavity that is surrounded by twelve bridging oxygen atoms. The A cations are situated within this cavity; the actual position assumed by the A-type cation and the number and configuration of the surrounding anions to which it is bonded are a function of local stereochemical requirements, and vary with the chemistry of the amphibole. The A cations thus provide additional linkage between adjacent double-chains orthogonal to the plane of the double-chain. Schematic projections are shown in Figures 9 and 11.

Choice of axes

The original crystal-structure determination for tremolite by Warren (1929) was referred to an I-centred cell and conformed to the early morphological convention of defining β as the acute angle between the X and the Z axes. Some confusion subsequently arose concerning this point (Whittaker & Zussman 1961). Warren's work was done before the introduction of the Hermann–Mauguin symbols, and the space group was reported as $2Ci$–3 using the Wyckoff notation. This was translated into the standard form $C2/m$ by later workers, but the unit-cell parameters were still given in the I-centred orientation. Current crystallographic convention for the monoclinic crystal system defines β as the obtuse angle between the X and Z crystallographic axes. Several later studies (Zussman 1955, Heritsch *et al.* 1960, Heritsch & Kahler 1960, Heritsch & Reichert 1960) reported atomic co-ordinates in an I-centred cell with β obtuse; in these studies, the signs of the z co-ordinates should be reversed.

Here, all crystallographic information has been standardized to a C-centred cell with β obtuse. Maintaining a right-handed set of crystallographic axes with β obtuse, Figure 10 summarizes the relationships between the I- and C-centred cells.

Principal structure-types

The extensive morphological investigations of the nineteenth century had shown that amphiboles occur in both monoclinic and orthorhombic varieties, and Warren's studies showed that these were related structures with space-group symmetries $C2/m$ and $Pnma$, respectively. More detailed work during the past twenty years has unearthed three more struc-

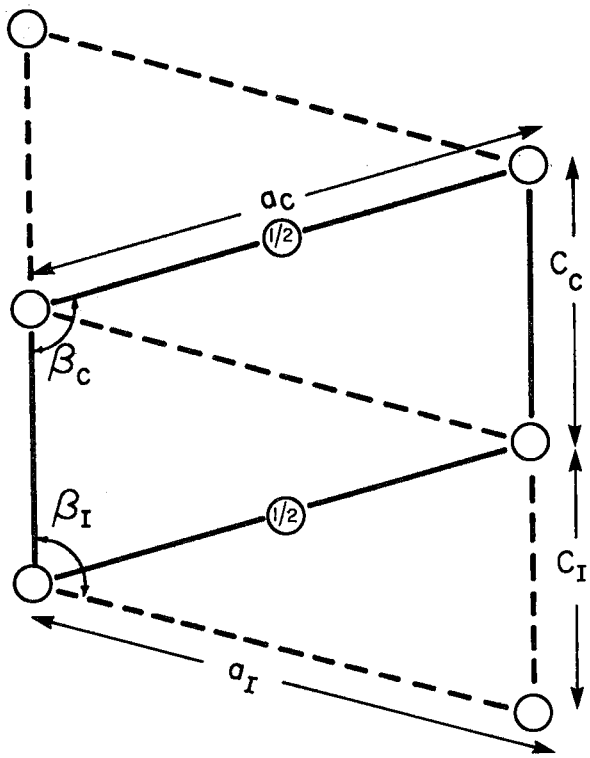

$$a_I = \sqrt{a_c^2 + c_c^2 + 2a_c c_c \cos \beta_c}$$

$$a_c = \sqrt{a_I^2 + c_I^2 + 2a_I c_I \cos \beta_I}$$

$$b_I = b_c$$

$$c_I = c_c$$

$$\sin \beta_I = \frac{a_c \sin \beta_c}{\sqrt{a_c^2 + c_c^2 + 2a_c c_c \cos \beta_c}}$$

$$\sin \beta_c = \frac{a_I \sin \beta_I}{\sqrt{a_I^2 + c_I^2 + 2a_I c_I \cos \beta_I}}$$

FIG. 10. The geometrical relationships between the *I*- and *C*-centred cells of the clinoamphiboles [modified from Whittaker & Zussman (1961)].

tural variants with different space-groups. Gibbs *et al.* (1960) reported the synthesis of protoamphibole, a new orthorhombic amphibole with space-group symmetry *Pnmn;* Gibbs (1964, 1969) subsequently refined the protoamphibole structure. Deer *et al.* (1963) postulated the existence of a magnesium-rich Fe–Mg–Mn amphibole with $P2_1/m$ symmetry. Bown (1966) subsequently reported such an amphibole, and the structure of a tirodite $P2_1/m$ was refined by Papike *et al.* (1969). Moore (1968a,b) reported the existence of a peculiar amphibole-like mineral from Långban, Sweden. The unit-cell dimensions and space group ($P2/a$) were found to be compatible with an amphibole-type structure but the chemical composition was not. Subsequent solution and refinement of the structure of this mineral (joesmithite) showed it to be a *bona fide* amphibole with a beryllosilicate double-chain (Moore 1969).

Site nomenclature in amphiboles

In order to facilitate interstructure comparison of structural features in the amphiboles, it is desirable to have a site nomenclature that differentiates between structure types but maintains some sort of congruence for analogous sites in different structures. There are also considerable advantages in a nomenclature that uses only upper-case characters and has no subscripts, superscripts or Greek letters; such a nomenclature is machine-readable and causes less type-setting problems. A site nomenclature should not involve symbols for chemical elements; it is confusing to have Fe occupying an Mg(1) site in a structure.

Numerous site-nomenclature schemes have been used in the various amphibole structure-types. Many of the earlier schemes are undesirable in that they use symbols of chemical elements, subscripts or Roman numerals. The more recent systems of site nomenclature are based on the scheme whereby the sites occupied by the T cations are denoted as T sites, the sites occupied by the C and B cations are denoted M sites, the site(s) occupied by the A cations is (are) denoted A sites, and all anion sites are denoted as O sites. This is the basis of the scheme used here. However, some changes to the

schemes of nomenclature used in some studies are necessary in order to satisfy the conditions outlined above. As will be shown later in this section, there are a large number of possible amphibole structures that could occur as ordered derivatives of currently known structures. A completely general site-nomenclature would satisfy the above restrictions for all these possible structures and would have the same type of structure as the nomenclature schemes that have been derived for the pyroxenes (Burnham *et al.* 1967) and the feldspars (Megaw 1956). Such a scheme would also be extremely cumbersome and is not really necessary unless numerous additional structural varieties are discovered. The scheme developed here is not as systematic but is convenient and satisfies the criteria cited above. The site nomenclature used by Robinson *et al.* (1973) and Hawthorne & Grundy (1973a, b) is adopted here for the $C2/m$ amphibole structure-type. The site nomenclatures for the other structural variants can be derived from this nomenclature by changes that correspond to the space-group differences of the structures involved. The difference between the monoclinic and orthorhombic amphiboles may be indicated by the presence or absence of parentheses in the site symbols. This is consistent with the current nomenclature of the *Pnma* amphiboles (Finger 1970b, Papike & Ross 1970), which is thus adopted in the current scheme. The site nomenclature of the *Pnmn* structure (Gibbs 1969) is changed; the parentheses are not used and the Si(1) and Si(2) sites become the T1 and T2 sites. For the $P2_1/m$ structure-type, parentheses

TABLE 8. SITE-NOMENCLATURE SCHEME FOR AMPHIBOLE STRUCTURE-TYPES

	C2/m	$P2_1/m$		P2/a		Pnma		Pnmn
tetrahedrally coordinated sites	T(1)	T(1A)	T(1B)	T(1)A	T(1)B	T1A	T1B	T1
	T(2)	T(2A)	T(2B)	T(2)A	T(2)B	T2A	T2B	T2
octahedrally coordinated sites	M(1)	M(1)		M(1)A	M(1)B	M1		M1
	M(2)	M(2)		M(2)A	M(2)B	M2		M2
	M(3)	M(3)		M(3)		M3		M3
cubic antiprismatic sites	M(4)	M(4)		M(4)A	M(4)B	M4		M4
[12] cavity*	A	A		A(2)		A		A
non-bridging anion sites	O(1)	O(1A)	O(1B)	O(1)A	O(1)B	O1A	O1B	O1
	O(2)	O(2A)	O(2B)	O(2)A	O(2)B	O2A	O2B	O2
	O(3)	O(3A)	O(3B)	O(3)		O3A	O3B	O3
	O(4)	O(4A)	O(4B)	O(4)A	O(4)B	O4A	O4B	O4
bridging anion sites	O(5)	O(5A)	O(5B)	O(5)A	O(5)B	O5A	O5B	O5
	O(6)	O(6A)	O(6B)	O(6)A	O(6)B	O6A	O6B	O6
	O(7)	O(7A)	O(7B)	O(7)		O7A	O7B	O7

*the more complex nomenclature used to describe the positional disorder of cations occupying this site is described in the section on the A site.

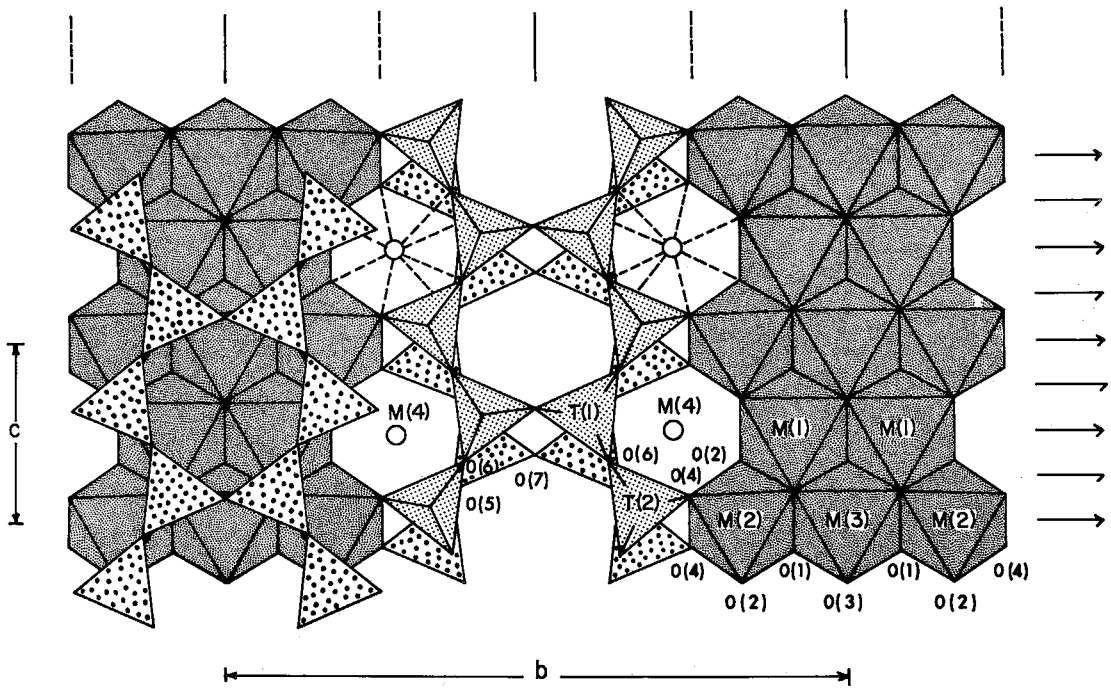

FIG. 11. The $C2/m$ amphibole structure projected on to (100); the space-group symmetry elements are shown.

were added to the nomenclature scheme of Papike *et al.* (1969, Fig. 2). The site-nomenclature scheme for the $P2/a$ structure (Moore 1969) does not resemble that of the other amphiboles and was completely revised. The site numbering was adjusted to correspond with numbering in the other amphibole structures; for the "pseudo-mirror equivalent" pairs of atoms, those with the smaller value of the y co-ordinate were labeled by addition of a suffix A, whereas those with the larger value of the y co-ordinate were labeled with the suffix B. Parentheses are used because this structure-type is monoclinic; however, in order to distinguish sites in this structure-type from similar sites in the $P2_1/m$ structure-type, the parentheses enclose the numbers only in the $P2/a$ structure-type. The relationship between $P2/a$ site-nomenclatures is shown explicitly in Appendix D. The sites of all the various structure-types are summarized in Table 8.

The C2/m amphibole structure

This is the most common of the amphibole structure-types, suggesting that this must be the most flexible, or chemically compliant, of these structures. A schematic polyhedral representation of this structure-type is shown in Figure 11. There are three nonbridging anions: O(1), O(2) and O(4); of these, O(1) and O(2) are apical oxygen atoms and O(4) is a basal oxygen. There are three bridging anions: O(5), O(6) and O(7); all of these are basal oxygen atoms, and O(5) and O(6) bridge along the length of the $(T_4O_{11})_\infty$ double-chain, whereas O(7) is the anion that links the two pyroxene-like components of the double chains together. In addition, there is the O(3) anion that is bonded to three octahedrally co-ordinated cations; the O(3) position may be occupied wholly or in part by OH, F, Cl or O^{-2}. These anions are arranged in layers parallel to the (100) plane; these layers are not close-packed but show a simple relationship to close-packed arrangements (see section on rotated-chain models).

There are two unique cation-sites with pseudotetrahedral co-ordination, the T(1) and T(2) sites, both of which have point symmetry 1. The T(1) site is co-ordinated by three bridging and one nonbridging anions, whereas the T(2) site is co-ordinated by two bridging and two nonbridging anions. There is an alternation of T(1) and T(2) tetrahedra along the length of the chain, and thus all chain linkages in this direction are of the type T(1)–(2). Conversely, the cross-chain linkage is of the type T(1)–T(1), as required by the mirror symmetry of the chain. These characteristics of the double chain have significant implications regarding the relative ordering of cations over the nonequivalent tetrahedrally co-ordinated sites in the structure. As in apparent from Figure 11, the double-chain element of the structure is not fully extended [O(5)–O(6)–O(5)$\neq$180°]. The ideal double-chain configuration is a series of linked hexagonal rings of tetrahedra. Deviations from this ideal hexagonal aspect impose a ditrigonal aspect to the double chains and can be thought of as arising from coupled rotations of the individual tetrahedra around axes defined by their T–O (apical) bonds. This deviation from the extended configuration varies with amphibole composition, and is one of the principal mechanisms whereby the double chain maintains dimensions commensurate with the octahedral strip.

There are three unique sites with pseudo-octahedral co-ordination, the M(1), M(2) and M(3) sites; the point symmetry of the M(1) and M(2) sites is 2 and the point symmetry of the M(3) site is $2/m$. Both the M(1) and M(3) sites are co-ordinated by four oxygen atoms and two O(3) anions; around the M(1) site, the O(3) anions are in a *cis* arrangement, whereas around the M(3) site they are in a *trans* arrangement. The M(2) site is co-ordinated by six oxygen atoms, and is situated at the margin of the octahedral strip. These three sites differ significantly in next-nearest-neighbor configuration, and thus afford great opportunity for differential ordering of C-type cations in this structure-type. Where such ordering produces octahedra of disparate sizes, the linkage requirements between the octahedral strip and the tetrahedral chain are more complex than adjustment to a simple dimensional misfit. In these cases, the tetrahedra of the double chain tilt to provide differential separations of the apical oxygen atoms co-ordinating these octahedra. As is apparent from Figure 16, the amphibole structure may be considered as an ordered stacking sequence along X of alternate layers of octahedra and tetrahedra. Because the apical oxygen atoms of the tetrahedral layers are providing the octahedral co-ordination of the octahedral layers, there is a stagger of $c/3$ between adjacent tetrahedral layers. For the $C2/m$ structure-type, this stagger is always in the same direction, as is depicted in Figure 16.

There is one unique cation-site surrounded by eight anions, the M(4) site with point symmetry 2. The anions are arranged in a distorted

square antiprism, but the actual cation co-ordination may vary with cation occupancy. The M(4) site is situated at the periphery of the octahedral strip and is occupied by the B-type cations of the standard formula. The cation occupancy of this site is the primary feature upon which the current nomenclature scheme of the amphiboles is based and is a major factor in the crystal chemistry of the amphiboles. The M(4) site differs from the octahedrally co-ordinated sites in that it is co-ordinated by both nonbridging and bridging anions. Inspection of Figure 11 shows that the details of the M(4) cation co-ordination are related to the ditrigonal aspect of the double chain. Between the back-to-back chains is a large cavity surrounded by twelve anions, in the centre of which is the A site, with point symmetry $2/m$. This site may or may not be occupied depending on the chemical composition of the amphibole. Detailed studies have shown that the cation occupying this cavity is positionally disordered off the centre of symmetry. The twelve anions surrounding the A site are all bridging anions, and form two ditrigonal rings on opposite sides of the cavity (Fig. 11). Because of the space-group symmetry of this structure-type, these ditrigonal rings point in opposite directions. This has important implications concerning the co-ordination of the cations occupying the cavity.

The $P2_1/m$ amphibole structure

This structure-type is restricted to magnesium-rich Fe–Mg–Mn amphiboles. Single-crystal X-ray-diffraction studies have confirmed this space-group for some samples of magnesio-cummingtonite and tirodite. Woensdregt & Hartman (1969) reported a hornblende with $P2_1/m$ symmetry intergrown with magnesio-cummingtonite $P2_1/m$; this seems unlikely in view of current ideas on the reasons for the existence of the $P2_1/m$ amphibole structure. A schematic polyhedral representation of this structure-type projected down X sin β is shown in Figure 12. There are six nonbridging anions: O(1A), O(2A), O(4A), O(1B), O(2B) and O(4B); of these, O(4A) and O(4B) are basal oxygen atoms and the remainder are apical oxygen atoms. There are six bridging anions: O(5A), O(6A), O(7A), O(5B), O(6B) and O(7B); all of these are basal oxygen atoms, with O(7A) and O(7B) cross-linking the double chains and the remainder bridging along the length of the $(T_4O_{11})_\infty$ double chains. In addition, there are two anion

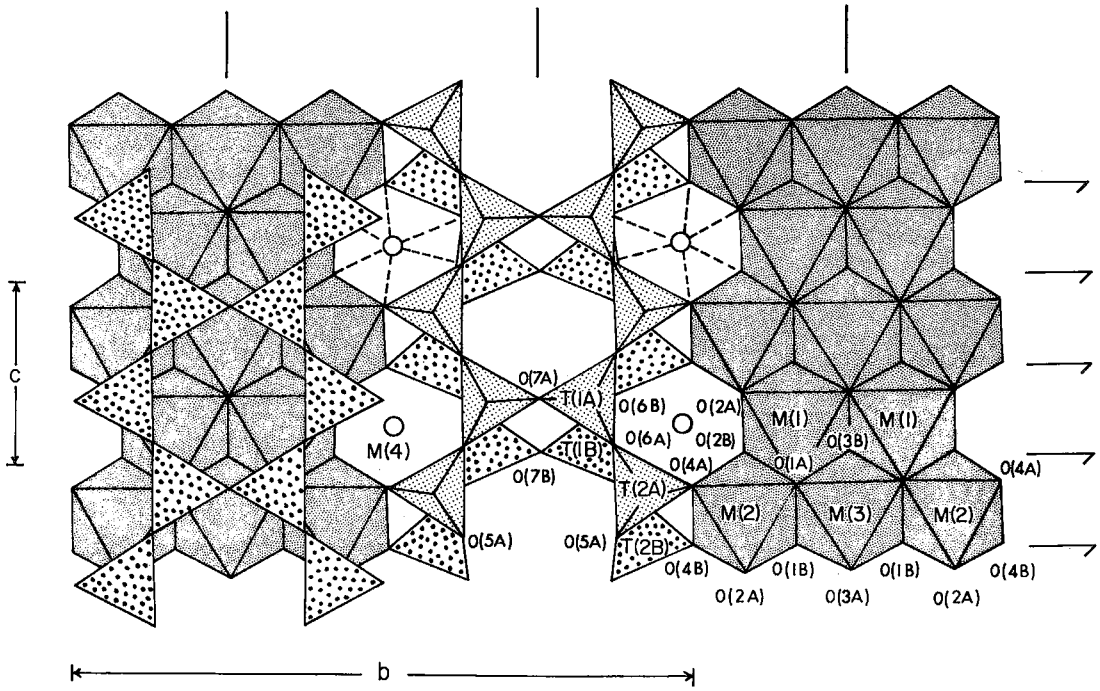

FIG. 12. The $P2_1/m$ amphibole structure projected on to (100); the space-group symmetry elements are shown.

positions, O(3A) and O(3B), that are co-ordinated to three octahedrally co-ordinated cations; these positions are generally occupied by OH in this structure-type.

There are four unique cation-sites with pseudo-tetrahedral co-ordination, the T(1A), T(2A), T(1B) and T(2B) sites, all of which have point-symmetry 1. The details of their co-ordination are similar to the co-ordination of the corresponding sites in the $C2/m$ structure-type, but the back-to-back double chains are crystallographically nonequivalent, and are designated the A and B chains. The B chain shows a much greater deviation from the extended chain configuration than does the A chain, with the average chain kinking being similar to that found in structures of similar composition with $C2/m$ symmetry. Cations labeled A always bond to anions labeled A, and likewise for the B-labeled cations. The double chains in this structure still have mirror symmetry and retain the same linkage configurations as the $C2/m$ structure in regard to the labeling of the atoms of the chains.

There are three unique sites with pseudo-octahedral co-ordination, the M(1), M(2) and M(3) sites; the point-symmetry of the M(1) and M(2) sites is 1 and the point-symmetry of the M(3) site is m. The relative configuration of these sites and their co-ordinating anions is similar to the corresponding sites in the $C2/m$ structure; note that the anions on one side of the octahedral strip are A-type anions, whereas the anions on the other side of the octahedral strip are B-type anions. Whereas there are two types of tetrahedral double-chain in this structure-type, there is only one type of octahedral strip.

At the margins of the octahedral strip is the M(4) site, with point-symmetry 2, surrounded by eight anions arranged in a very distorted square antiprism. The cations occupying the M(4) site may not bond to all of the surrounding anions; indeed, the existence of this structure-type seems to hinge on the bonding requirements of the M(4) cation(s). Between the back-to-back A and B chains is the A site, with point-symmetry m. This site is identified by analogy with other structure-types, as it is unoccupied in all $P2_1/m$ structures examined thus far.

The P2/a amphibole structure

Only one representative of this structure-type has so far been discovered. Joesmithite is a natural beryllosilicate amphibole whose unusual structure can be related to its unusual

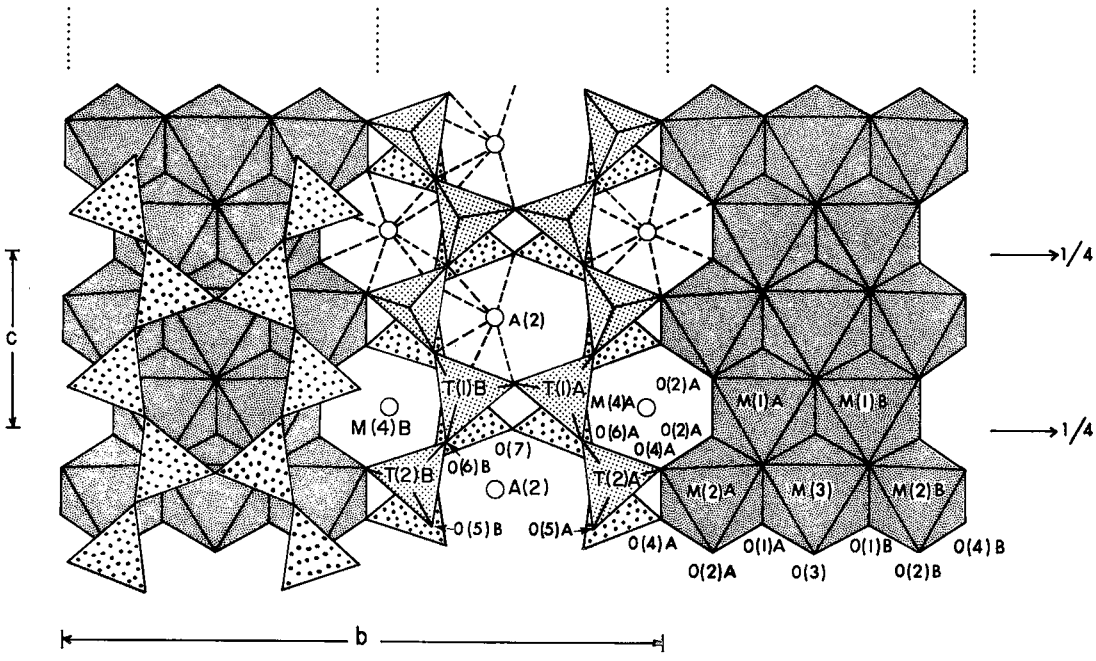

FIG. 13. The $P2/a$ amphibole structure projected on to (100); the space-group symmetry elements are shown.

chemical composition. A schematic polyhedral representation of joesmithite is shown in Figure 13. Note that the nomenclature of sites is different from that used by Moore (1969). There are six nonbridging anions: O(1)A, O(2)A, O(4)A, O(1)B, O(2)B and O(4)B; of these, O(4)A and O(4)B are basal oxygen atoms and the remainder are apical oxygen atoms. There are five bridging anions: O(5)A, O(6)A, O(5)B, O(6)B and O(7); all of these are basal oxygen atoms, O(7) cross-links the double chain and the remainder bridge along the length of the double chain. In addition, there is the O(3) anion position that is co-ordinated to three octahedrally co-ordinated cations and is occupied by OH.

There are four unique cation-sites with pseudotetrahedral co-ordination, the T(1)A, T(2)A, T(1)B and T(2)B sites, all of which have point-symmetry 1. The details of their co-ordination are similar to the co-ordination of the corresponding sites in the $P2_1/m$ structure-type. Whereas in the $P2_1/m$ and *Pnma* structures, the four unique tetrahedrally co-ordinated sites give rise to two distinct tetrahedral double-chains, the four unique tetrahedra in the $P2/a$ structure form just one double-chain.

There are five unique sites with pseudo-octahedral co-ordination, the M(1)A, M(2)A, M(1)B, M(2)B and M(3) sites, all of which have point-symmetry 2. The relative configuration of these sites and of their co-ordinating anions is similar to the analogous sites in the $C2/m$ structure. Cations denoted by A and B bond to A- and B-type anions, respectively. There is only one type of octahedral strip. At the margins of the octahedral strip are the M(4)A and M(4)B sites, both of which have point-symmetry 2. The anions surrounding each site are arranged in a distorted square antiprism, with all the anions bonded to the central cation in joesmithite. Sandwiched between the back-to-back double chains is the A-site cavity, surrounded by twelve anions. In joesmithite, this cavity is fully occupied by divalent cations that assume an ordered off-centre position, the A(2) site. This displacement is along the two-fold axis towards the T(1)B site that contains Be.

The Pnma amphibole structure

This is the only structure-type found thus far for naturally occurring orthorhombic am-

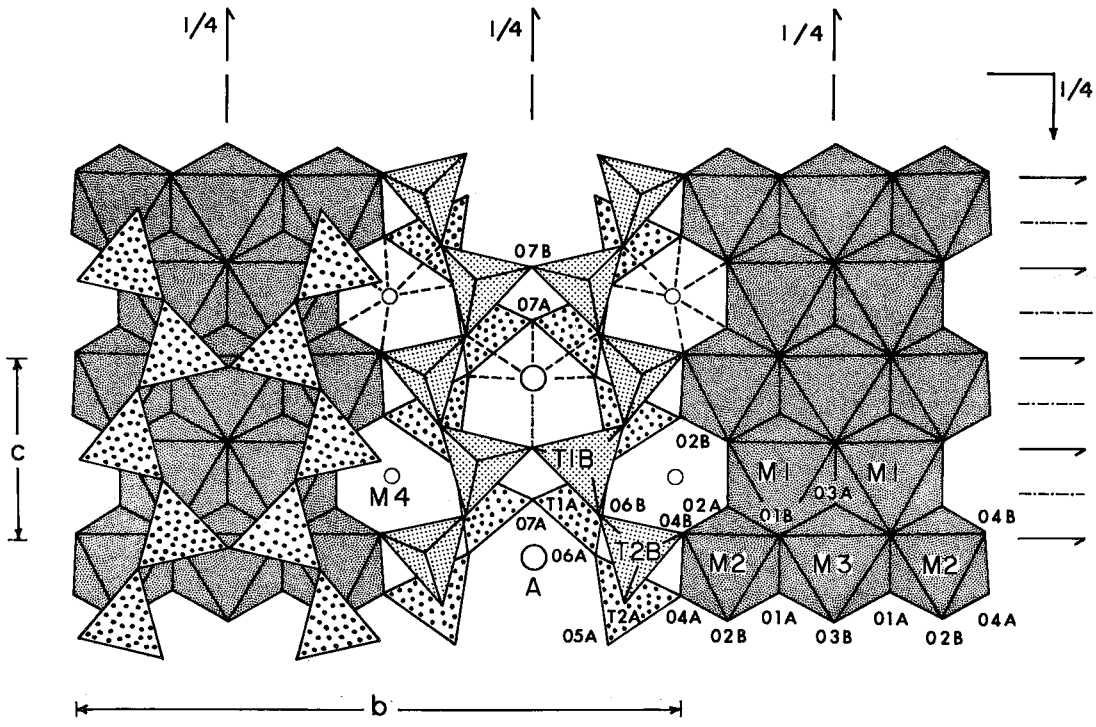

FIG. 14. The *Pnma* amphibole structure projected on to (100); the space-group symmetry elements are shown.

phiboles. A schematic polyhedral representation of this structure-type is shown in Figure 14. There are six nonbridging anions: O1A, O2A, O4A, O1B, O2B and O4B; of these, O4A and O4B are basal oxygen atoms and the rest are apical oxygen atoms. There are six bridging anions: O5A, O6A, O7A, O5B, O6B and O7B; all of these are basal oxygen atoms, with O7A and O7B bridging across the chains and the rest bridging along the length of the chains. In addition, there are the O3A and O3B anion positions, both of which are co-ordinated to three octahedrally co-ordinated cations and are occupied by OH, F, Cl or O^{2-}.

There are four unique cation-sites with pseudotetrahedral co-ordination, the T1A, T2A, T1B and T2B sites, all of which have point-symmetry 1. The T1A and T1B sites are co-ordinated by three bridging and one nonbridging anions and the T2A and T2B sites are co-ordinated by two bridging and two nonbridging anions. The cations in sites designated A and B are co-ordinated, respectively, to A- and B-type anions only. There are two crystallographically distinct double chains, the A chain and the B chain, that are constituted from A- and B-type atoms, respectively. Both A and B chains have mirror symmetry, and all of the intrachain linkages are analogous to those in the $C2/m$ structure-type. There is generally a significant difference in the degree of ditrigonal rotation of each chain, the B chain being more kinked than the A chain, with <O5–O6–O5> values of 153.6 and 165.1,° respectively, for the structures of Appendix C.

There are three unique sites with pseudo-octahedral co-ordination, the M1, M2 and M3 sites, with point-symmetries 1, 1 and *m*, respectively. Apart from the differences in point-symmetry, the co-ordination of these sites is similar to that of the corresponding sites in the $C2/m$ structure. The anions on one side of the octahedral strip are A-type anions and on the other side, B-type anions. Thus there is only one type of octahedral strip in this structure-type.

At the edges of the octahedral strip is the M4 site, with point-symmetry 1, surrounded by eight anions. The actual co-ordination number almost certainly varies with cation occupancy of this site, and is possibly one of the more important factors in the occurrence of this structure-type. The cations occupying this site may bond to bridging anions of both the A

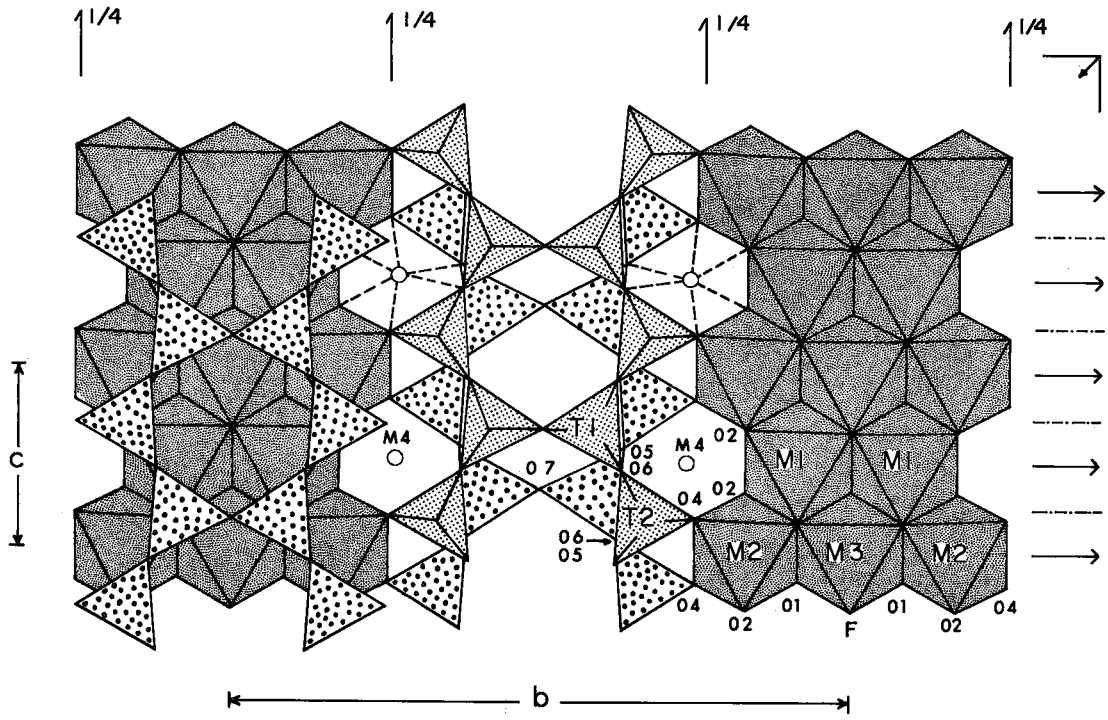

FIG. 15. The *Pnmn* amphibole structure projected on to(100); the space-group symmetry elements are shown.

and the B tetrahedral double-chains; thus the cations occupying this site have great flexibility with regard to the possible co-ordination geometry they assume. Between the back-to-back A and B double-chains is the A site, point-symmetry *m*, that is co-ordinated by six bridging anions. This site may or may not be occupied depending on the chemical composition of the amphibole. Unlike the *C*2/*m* amphibole structure, there seems to be no significant positional disorder of the cations occupying this position in amphiboles of the *Pnma* structure-type.

The Pnmn amphibole structure

No naturally occurring amphiboles with this structure-type have yet been found. Protoamphibole (Gibbs *et al.* 1960) is a synthetic amphibole with orthorhombic symmetry, and the only representative of this structure-type known. A schematic polyhedral representation of this structure-type is shown in Figure 15. There are three nonbridging anions: O1, O2 and O4; the latter is a basal oxygen and the other two are apical oxygen atoms. There are three bridging anions: O5, O6 and O7; all of these are basal oxygen atoms, with O7 bridging across and O5 and O6 bridging along the tetrahedral double-chain. In addition, there is the O3 anion position, which is co-ordinated to three octahedrally co-ordinated cations and is occupied by F in protoamphibole. There are two unique cation-sites with pseudotetrahedral co-ordination, the T1 and T2 sites, with point-symmetry 1. The T1 site is co-ordinated by three bridging and one nonbridging anions and the T2 site is co-ordinated by two bridging and two nonbridging anions. There is only one symmetrically distinct tetrahedral double chain in this structure-type, with distinct tetrahedra alternating along the chain.

There are three unique sites with pseudo-octahedral co-ordination, the M1, M2 and M3 sites, with point-symmetry 2, 2 and 2/*m*, respectively. The co-ordination of these sites is similar to the analogous sites in the *C*2/*m* amphibole structure, and there is only one symmetrically distinct octahedral strip. At the edge of the octahedral strip is the M4 site, with point-symmetry 2, surrounded by eight anions, only six of which are bonded to the central M4 cation. Although only co-ordinated by six anions, the M4 site still differs significantly from the pseudo-octahedrally co-ordinated M1, M2 and M3 cation sites of the octahedral strip, in that its central cation bonds both to non-bridging and bridging anions. Between the back-to-back double chains is a large cavity surrounded by twelve anions, in the centre of which is the A site with point-symmetry 2/*m*. According to the chemical composition of protoamphibole, this site should be almost completely occupied by Li; however, Gibbs (1969) could not locate the position of Li (a very weak X-ray scatterer) in the structure refinement, and suggested that it is positionally disordered within this cavity.

TABLE 9. OBSERVED AMPHIBOLE SPACE-GROUPS AND REPRESENTATIVE STRUCTURES

C2/m	calcic amphiboles, sodic-calcic amphiboles, alkali amphiboles, monoclinic Fe-Mg-Mn amphiboles
$P2_1/m$	magnesio-cummingtonite
P2/a	joesmithite
Pnma	orthorhombic Fe-Mg-Mn amphiboles, holmquistite
Pnmn	protoamphibole

Space-group variations in amphiboles

There are at present five known structural variants of amphiboles, details of which are given above. Representative amphiboles with these structure-types are listed in Table 9. In regard to the existence of other possible structure-types, it is instructive to consider the *P*2/*a* and $P2_1/m$ structures. The *P*2/*a* structure has the same topological arrangement as the *C*2/*m* structure, but a different topochemical arrangement. It is the difference in cation ordering that leads to the different space-group; there is no major change in the shape or size of the unit cell, and the space group *P*2/*a* is a subgroup of the space group *C*2/*m*. The $P2_1/m$ structure has the same topochemical arrangement as the *C*2/*m* structure. Whether or not the topological arrangement is the same is a moot point. However, we can understand the difference in symmetry between these two structure-types as a release of symmetry constraints to allow local relaxation in the structure; there is no major topological change in the structure type, such as a change in stacking sequence. Again, the space group $P2_1/m$ is a subgroup of the space group *C*2/*m*. Thus we can identify the *C*2/*m*, *Pnma* and *Pnmn* as principal structure-types in the amphi-

TABLE 10. SUBGROUPS OF C2/m, Pnma AND Pnmn

*C2/m	*Pnma	*Pnmn
Monoclinic (Y)+	Orthorhombic	Orthorhombic
$P2_1/a$	$Pn2_1a$	Pn2n
*$P2_1/m$	$Pnm2_1$	$Pnm2_1$
*P2/a	$P2_1ma$	$P2_1mn$
P2/m	$P2_12_12_1$	$P2_12_12_1$
Cm	Monoclinic (X)	Monoclinic (X)
C2	$P2_1/n$	$P2_1/n$
$P2_1$	$P2_1$	$P2_1$
P2	Pn	Pn
Pa	Monoclinic (Y)	Monoclinic (Y)
Pm	$P2_1/m$	P2/m
Triclinic	$P2_1$	P2
$C\bar{1}$	Pm	Pm
C1	Monoclinic (Z)	Monoclinic (Z)
$P\bar{1}$	$P2_1/a$	$P2_1/n$
$P\bar{1}$	$P2_1$	$P2_1$
P1	Pa	Pn
	Triclinic	Triclinic
	$P\bar{1}$	$P\bar{1}$
	P1	P1

*reported as amphibole space-groups

+signifies unique axis

boles, as none of these can be considered as simple subgroup-derivatives of the other(s). All possible space-groups for amphibole structures derivative from the *C2/m, Pnma* and *Pnmn* structures without a change in shape or size of the unit cell are subgroups of these space groups. The possible supergroups of these three space-groups are not consistent with the amphibole structure without a change in shape and size of the unit cell, and thus all possible space-groups may be derived from *C2/m, Pnma* and *Pnmn* by group reduction [for an introduction to group theory and symmetry, see Yale (1968)].

A space group G may be written as: $G = P \cdot Q$, where P is the primitive lattice group and Q is the factor group (Zachariasen 1945). Thus all space groups that are subgroups of G may be formed by taking the semidirect product of P and all subgroups of Q. For each of the space groups under consideration, the rank of Q is 8; thus the ranks of all relevant subgroups of Q are 4, 2 and 1. In each case, all elements of Q are binary and thus all subgroups, H, of Q with rank 2 are $(I \cdot e)$, where e is a nonidentity element of Q. All subgroups, F, of Q with rank 4 may then be derived from the relation: $H \cdot F = Q$.

Subgroups of *C2/m, Pnma* and *Pnmn* derived in this manner are listed in Table 10. The two $P\bar{1}$ space-groups listed as subgroups of *C2/m* are structurally distinct as there are two symmetrically distinct centres of symmetry in *C2/m*. This situation does not arise for $C\bar{1}$, as both centres of symmetry are elements of this space group. Other amphibole structure-types, in addition to the ones examined here, are possible. However, they involve a change in the shape and size of the unit cell or a change in the stacking sequence along the *X* axis.

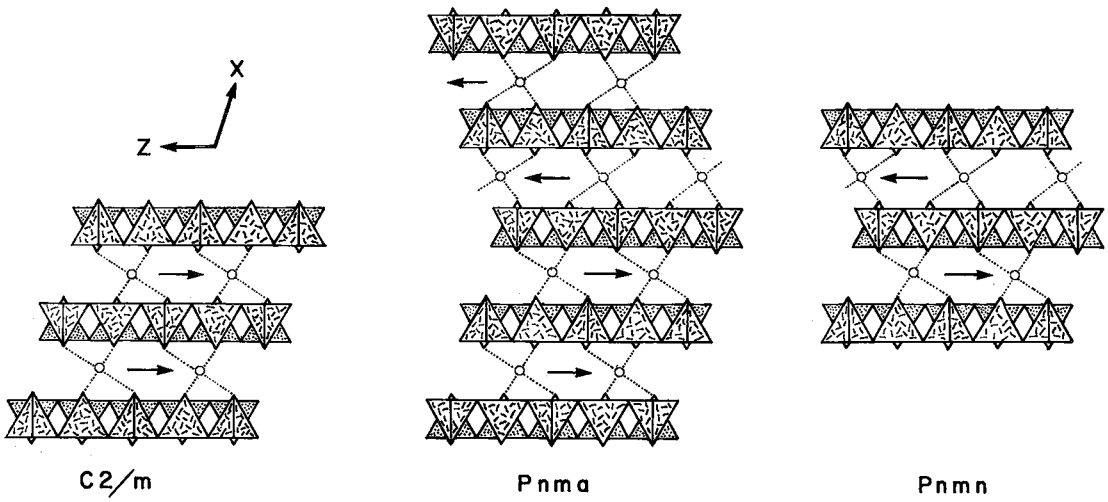

FIG. 16. Schematic representation of the stacking sequences of layers as projected down *Y* for the various amphibole structure-types (modified from Gibbs 1966); the $P2_1/m$ and $P2/a$ sequences are the same as for the *C2/m* structure type, and are not depicted here.

Amphiboles as layer structures

Amphiboles may be considered as ordered stacking sequences along X of alternate layers of octahedra and tetrahedra (Figs. 9 and 16). Because the apical oxygen atoms of the tetrahedral layers provide the octahedral co-ordination of the octahedral layers, there is a stagger of $\pm c/3$ between adjacent tetrahedral layers. For the monoclinic structure-types, this stagger is always in the same direction. The orthorhombic amphiboles require a regular reversal of this stagger in order that the resulting structures conform to the requirements of orthorhombic symmetry. For the *Pnma* structure-type, the stagger between adjacent tetrahedral layers is $(+c/3, +c/3, -c/3, -c/3)$, whereas for the *Pnmn* structure-type, the stacking-sequence stagger is $(+c/3, -c/3, +c/3, -c/3$. These relationships are summarized in Figure 16.

Model Structures

The amphibole structures are particularly amenable to analysis using fairly simple geometrical models. The differences among structure types and the geometrical responses of the structures to changing chemical composition can be profitably characterized in a simple manner. In addition, the same models can also be used to develop structural and chemographic relationships among the amphiboles and other common silicates, such as the pyroxenes and the micas. These approaches are not new; they were developed contemporaneously with the solution of the pyroxene, amphibole and mica structures. The relationship between the structures of diopside and tremolite was used in the solution of the tremolite structure (Warren 1929); the anthophyllite structure (Warren & Modell 1930b) was derived in a similar fashion from the structure of enstatite (Warren & Modell 1930a). Jackson & West (1930) further elaborated the structural and chemical relationships between the pyroxenes, amphiboles, micas and talc; their structural diagrams are essentially identical to the I-beam diagrams used today, and their dissection of the structures into chemically and structurally simpler units parallels current interpretations.

The essential feature of these models is that they recognize a basic unit that is larger than the individual atoms, and generally larger than single co-ordination polyhedra. Such units are called modules, and are based on perfectly regular (holosymmetric) co-ordination polyhedra. It should be emphasized that a specific module has integrity only within the bounds of the model in which it is recognized. Conversely, when working within the bounds of a specific model, it is important to recognize that the model may not give due emphasis to all of the features of the amphibole structure; indeed, if any one specific model did, there would be no need for any other models.

The extended-chain model

It is appropriate that this model be presented first as it is the original solution presented by Warren (1929) for the structure of tremolite. Warren & Modell (1930b) also gave an extended-chain model for the structure of anthophyllite. The basic features of the model, as given by

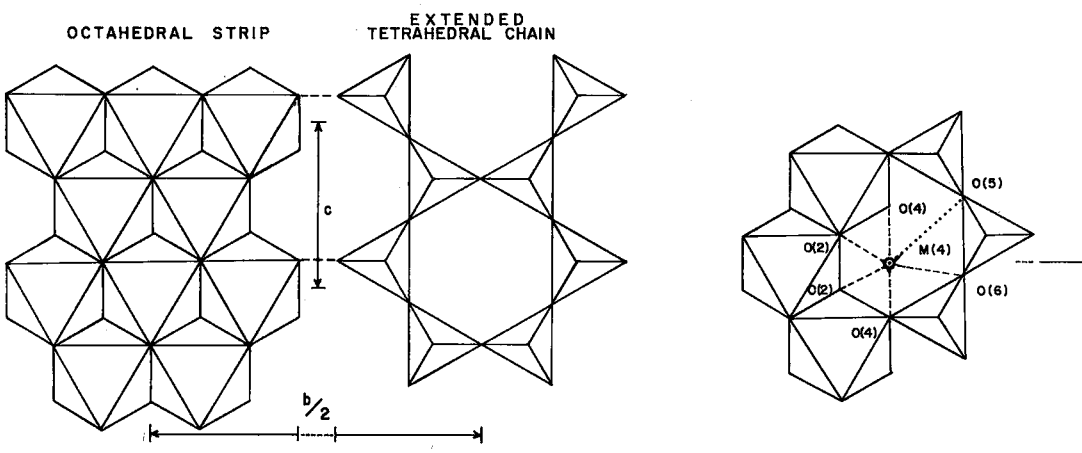

FIG. 17. The extended chain model of the amphibole structure [from Hawthorne 1979)]; the octahedral strip and the tetrahedral double-chain link in the Y direction as indicated by the broken lines.

TABLE 11. METRIC COORDINATES OF THE IDEAL C2/m AMPHIBOLE STRUCTURE (UPPER SET) COMPARED WITH THE METRIC COORDINATES OF GRUNERITE(22)

Atom	x	y	z
O(1)	0.1340	0.0833	0.1667
	0.1120	0.0882	0.1631
O(2)	0.1340	0.1667	0.6667
	0.1253	0.1735	0.6679
O(3)	0.1340	0	0.6667
	0.1147	0	0.6612
O(4)	0.3660	0.2500	0.6667
	0.3839	0.2416	0.6272
O(5)	0.3660	0.1250	-0.0833
	0.3483	0.1275	-0.0767
O(6)	0.3660	0.1250	0.4167
	0.3478	0.1182	0.4246
O(7)	0.3660	0	0.1667
	0.3376	0	0.1454
T(1)	0.3080	0.0833	0.1667
	0.2867	0.0836	0.1649
T(2)	0.3080	0.1667	0.6667
	0.2993	0.1667	0.6675
M(1)	0	0.0833	1/2
	0	0.0878	1/2
M(2)	0	0.1667	0
	0	0.1794	0
M(3)	0	0	0
	0	0	0
M(4)	0	0.2500	1/2
	0	0.2574	1/2

$a\sin\beta = 4\sqrt{2}\ (a+d)/\sqrt{3}$

$b = 12a$

$c = 2\sqrt{3}a$

$\beta = \tan^{-1} 1/\sqrt{2}\ (2+\sqrt{3})$

	Ideal structure	Grunerite (22)	Diff (%)
$a\sin\beta$	9.307Å	9.358Å	0.6
a	9.481	9.564	0.9
b	18.240	18.393	0.8
c	5.265	5.339	1.4
β	101°	101.9°	0.9
V	893.7Å^3	918.9Å^3	2.7

Hawthorne (1979), are shown in Figure 17. There are two basic modules, the octahedral strip and the tetrahedral double-chain, that are ideal geometrical analogues of the corresponding units in the *C2/m* amphibole structure (Fig. 11). In particular, the bridging anions along the length of the double-chain have a linear arrangement; this is the characteristic feature of the extended-chain model. In Figure 17, the cross-linkage in the *Y* direction is indicated by the broken lines. The dimensional requirements of both this cross-linkage and linkage between adjacent units in the *X* direction is an octahedral bond-length–tetrahedral bond-length ratio of 4:3. Using the ionic radii of Shannon (1976), an ideal T(Si)–O bond-length may be calculated; a value of 1.62 Å results, in reasonably good agreement with mean tetrahedral bond-lengths in non-^{iv}Al amphiboles. Calculating the corresponding mean octahedral bond-length for this extended-chain model and subtracting the mean anion radius gives a value of 0.78 Å as the cation size necessary for complete linkage; this value corresponds to [6]-co-ordinate Fe^{2+}.

Atomic co-ordinates may be derived for this ideal model of the *C2/m* structure. In order to facilitate comparison with real structures with different β angles, it is more convenient to work in an orthogonal co-ordinate system. The axes used to derive the co-ordinates of the ideal structure are $X\sin\beta$, *Y* and *Z*; these co-ordinates are listed in Table 11. Comparison with refined *C2/m* amphiboles (transformed to this axial system) shows grunerite(22) to have the closest agreement with the idealized extended structure, closely followed by tirodite (28). This is in accord with the conclusion that the ideal structure can incorporate a cation the size of Fe^{2+} without any necessary distortion in order to geometrically maintain intermodule linkage. The cell dimensions for this ideal structure also compare favorably with those of grunerite(22), the mean deviation being less than 1% (Table 11).

Whittaker (1949) showed that in the structure of magnesio-riebeckite(3), the double-chain module has a significant deviation away from this extended-chain configuration. This has since been found to be characteristic of all refined amphibole structures. From qualitative considerations, Hawthorne & Grundy (1973b) and Robinson *et al.* (1973) proposed that the amount of "kinking" of the double chain is a function of the ^{iv}Al content of the amphibole. One of the principal uses of the extended-chain model was to examine how the two modules of the structure maintained linkage with variation in chemical composition. With regard to the ideal model of Figure 17, departure of the octahedral–tetrahedral bond-length ratio from its ideal value of 4/3 must lead to some distortion from the ideal module-configuration if the intermodule linkage is to be maintained. If the bond-length ratio exceeds 4/3, linkage cannot be maintained without deviation from ideal geometry of the polyhedra in at least one of the modules. It is interesting that the mean octahedral – mean tetrahedral bond-length ratio in refined amphiboles does not seem to exceed 4/3. If the bond-length ratio is less than 4/3, linkage may be maintained by a kinking or rotation of the double-chain module away from the extended configuration. If θ is the O(br)–O(br)–O(br) angle along the length of the double

chain, simple geometrical arguments show that the condition

$$\langle M\text{–}O\rangle = \frac{4}{3}\langle T\text{–}O\rangle \sin(\theta/2) \qquad (1)$$

is required for complete articulation.

In terms of real amphibole structures, the angle θ is best calculated as the weighted mean of all O(br)–O(br)–O(br) angles projected on to (100). It is much simpler to use the O(5)–O(6)–O(5) angle, and the relationships are not particularly influenced by this approximation. Figure 18 shows the variation in the tetrahedral chain rotation as a function of the mean octahedral – mean tetrahedral bond-length ratio; a linear correlation occurs, but the deviation of the glaucophanes and taramites from the general trend suggests that the relationship is perturbed by such factors as the type of M(4) cation. Such scatter as is displayed in Figure 18 is not surprising considering the ideality of the model; however, its utility in rationalizing the general features of the octahedral strip and tetrahedral double-chain is apparent (*cf.* Veblen & Burnham 1978).

Although Figure 18 shows a fairly well-developed correlation, the relationship systematically deviates from equation (1). This reflects the fact that real structures are distorted from the ideal modules of Figure 17, as crystal-chemical factors cause changes from ideal geometry of polyhedra that also influence the articulation requirements of the modules themselves. Cation–cation repulsion in the octahedral strip shortens shared edges, with the concomitant lengthening of unshared edges; thus, all octahedral edges involved in the intermodular linkages are extended, which will tend to compensate for the substitution of larger tetrahedral cations or smaller octahedral cations. Conversely, T–O(br) bonds tend to be longer than T–O(nbr) bonds, which extends the dimensions of the double-chain module in the directions of polymerization and offsets the cation–cation repulsion effect in the octahedral strip. The fact that the trend of Figure 18 lies below the ideal relationship suggested by equation (1) indicates that lengthening of the linking O–O octahedral edges is the more dominant

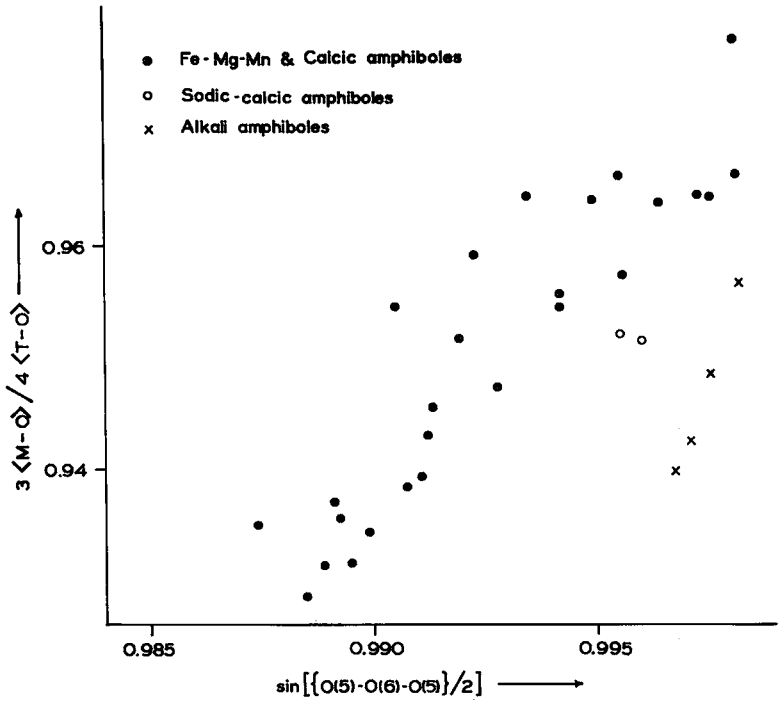

FIG. 18. The variation in $3\langle M\text{–}O\rangle/4\langle T\text{–}O\rangle$ with double-chain rotation as measured by the O(5)–O(63–O(5) angle for the *C*2/*m* amphiboles [modified from Hawthorne (1979)]. ○ Fe–Mg–Mn amphiboles; ● calcic amphiboles; □ sodic-calcic amphiboles; ■ alkali amphiboles.

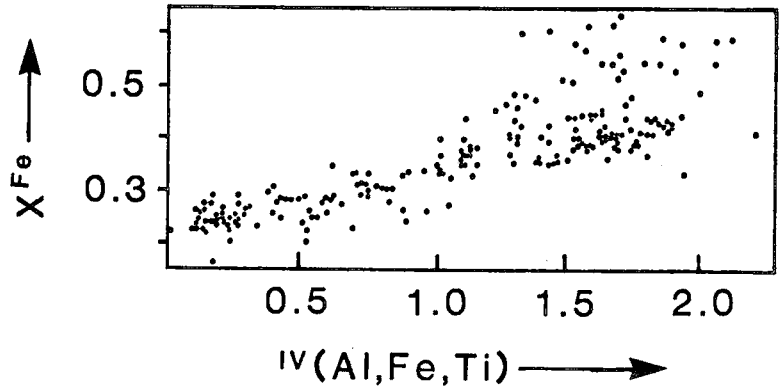

FIG. 19. The variation in Fe/(Fe+Mg) with ^{iv}Al for metamorphic amphiboles coexisting with biotite [after Gorbatschev (1977)].

effect. Other factors enter into the relative configuration of these two modules, but the simple picture presented above has some utility in the examination of structural response to changes in chemical composition, temperature and pressure.

In a given set of external conditions, this model would suggest that increasing substitution of larger cations at the tetrahedrally co-ordinated sites would be correlated with increasing size of cations at the octahedrally co-ordinated sites. For example, Figure 19 shows this to be the case for calcic amphiboles coexisting with biotite from granites and high-grade gneisses. This correlation is surprisingly good considering that such a relationship should be sensitive also to Na contents of M(4) and A, the K content of A and temperature variations.

This model also provides a crude framework in which to consider the relative maximum thermal stabilities of different amphiboles. It is well known that the rates of thermal expansion of cation polyhedra are some inverse function of mean cation–anion bond-valence. Hence the octahedral strip will expand faster than the tetrahedral double-chain upon heating; this has been verified by high-temperature crystal-structure refinements of amphiboles (Sueno *et al.* 1972a, 1973, Cameron *et al.* 1973a, b). Thus it is tempting to ascribe the breakdown of an amphibole to that point where the octahedral strip can no longer link to the tetrahedral chain. Using this argument, small octahedrally co-ordinated cations, substitution of F for OH at O(3) and large tetrahedrally co-ordinated cations would promote higher thermal stability; this tends to be the case, although the presence of B- and A-type cations are also of importance.

Rotated-chain models

These have been used quite frequently as models for both amphibole and pyroxene structures, but the emphasis adopted by different workers varies considerably. The model was developed by Thompson (1970) as a general way of looking at pyroxenes, amphiboles and micas. Following Pauling (1930) and Jackson & West (1930), Thompson (1970) pointed out that these three groups of structures could be regarded as alternating layers of octahedra and tetrahedra parallel to (100) in pyroxene and (001) in micas. Such models can maintain their linkage as the relative sizes of the constituent polyhedra vary, by rotation of the tetrahedra in the double chain about an axis through the T–O bond orthogonal to the layers. Rotation of the tetrahedra 30° in either sense from the extended configuration brings the oxygen atoms into a close-packed array in which all the cation polyhedra analogous to those in the real structures become regular octahedra or tetrahedra. Two senses of rotation may be defined:
(i) *S rotation:* rotation brings the triangular tetrahedral face orthogonal to the rotation axis into the same orientation as that of the nearest parallel octahedral faces of the octahedral strip to which the tetrahedron is linked by the terminal anion on the rotation axis.
(ii) *O rotation:* rotation brings the triangular tetrahedral face orthogonal to the rotation axis into the opposite orientation to that of the nearest parallel octahedral faces of the octahedral strip to which the tetrahedron is linked by the terminal anion on the rotation axis.

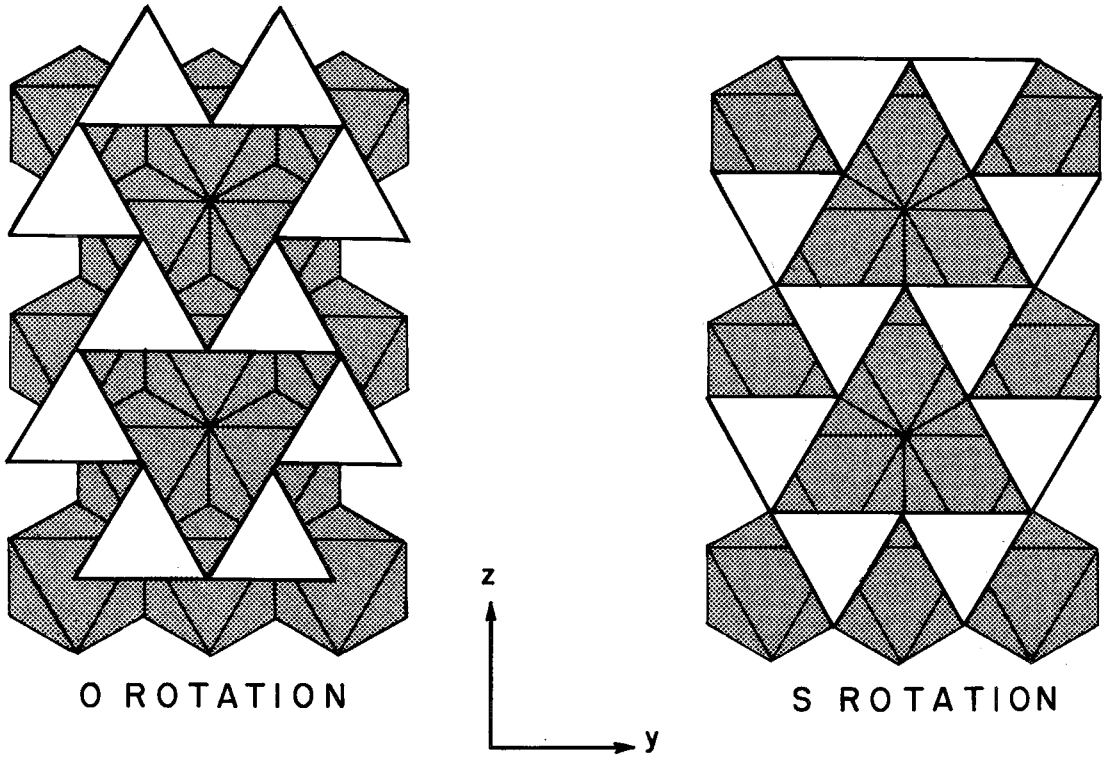

FIG. 20. Idealized octahedral strip and tetrahedral chain showing complete O-rotations (left) and S-rotations (right) [after Papike & Ross (1970)].

These two types of rotation are illustrated in Figure 20. No symmetry operation can transform an O-rotated configuration into an S-rotated configuration. Complete S-rotation results in a hexagonal close-packed array of anions, whereas complete O-rotation results in a cubic close-packed array of anions. Complete rotation in either sense forms regular octahedra from the larger polyhedra surrounding the M(4) and A sites found in the normal structures; however, S rotation produces octahedra that share edges with the adjacent tetrahedra, whereas O rotation does not. This led Thompson to suggest that O rotations should be preferred in real crystals, as is the case. The absolute attitude of the rotated tetrahedra is a function of the geometry of the associated octahedral strips. Papike & Ross (1970) defined the orientation of the octahedral strip with respect to the crystallographic axes. One pair of faces on each octahedron is parallel to (100); the upper and lower triangular faces of each octahedron are oriented in opposite senses, but all faces on the same side of an octahedral strip have the same orientation. Following Papike & Ross (1970), a positively (+) directed strip is defined as one in which the lower triangular faces of a given octahedral strip (as viewed along $-X\sin\beta$) have one of their three apices pointing in the $+Z$ direction. Conversely, a negatively (−) directed strip has the same set of apices pointing in the $-Z$ direction. Thompson (1970) indicated that in this ideal model, the linkage requirements of adjacent modules limit the character of the rotations according to a parity rule that was defined as follows: "If two (such) tetrahedral strips are both rotated in the same sense, then the two octahedral strips (one above and one below the tetrahedral layer) to which they are joined across (100) must both have a "tilt" or "skew" of the same sense. If the rotations are in the opposite senses, then the tilts must be in opposite senses". The need for this rule in completely rotated ideal structures is shown in Figure 21, where it may be seen that structures violating the parity rule do not fit together. According to this parity rule, sequences showing both positive and negative octahedral strips should contain S rotations in addition to O rotations.

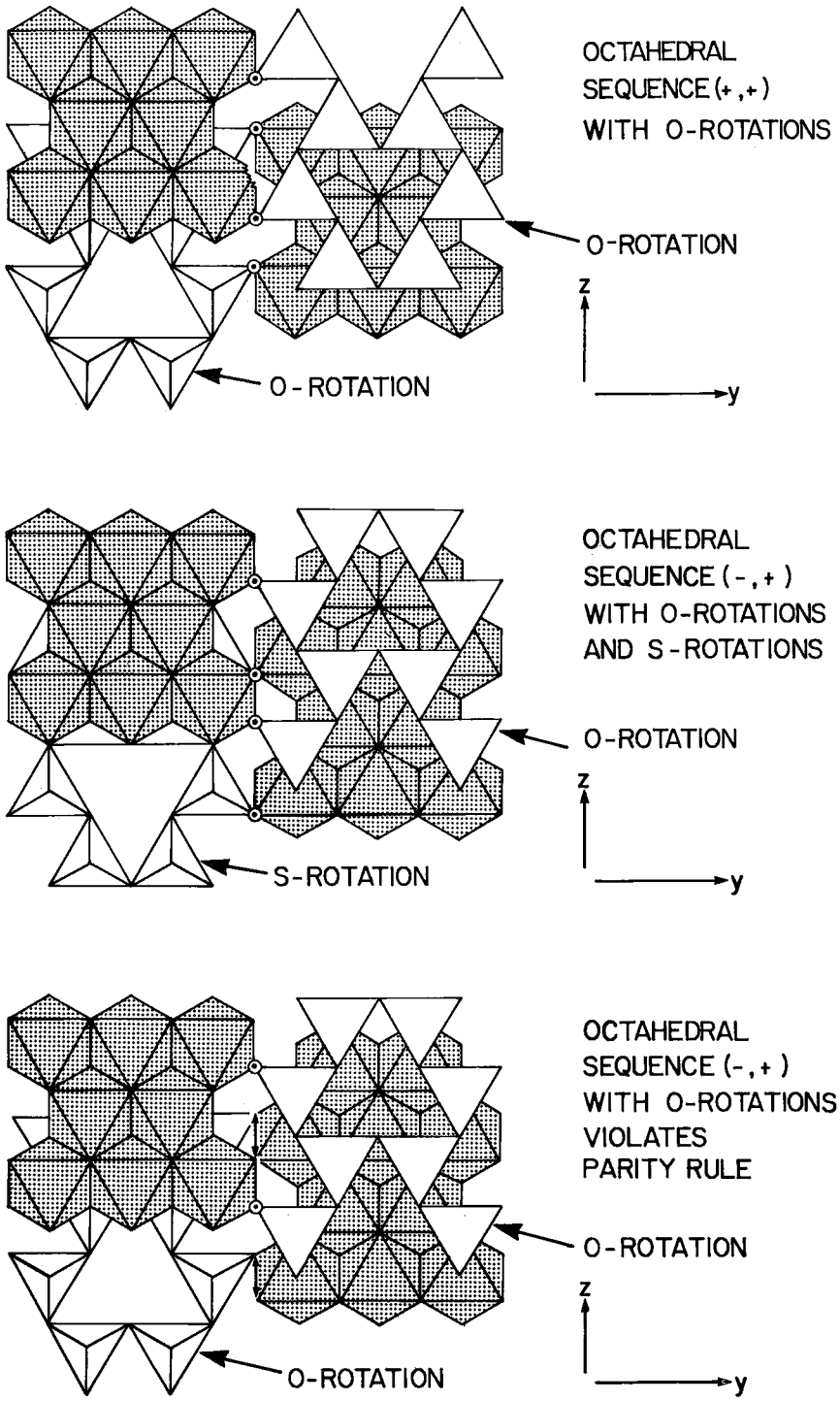

FIG. 21. Stacking sequences for ideal, completely rotated amphibole structures [after Papike & Ross (1970)]. The arrows in (c) denote the degree of mismatch between tetrahedra and octahedra where the parity rule is violated.

Real amphibole structures are more closely approximated by models with extended chains. The close-packed models may be considered as rotated-chain derivatives of the extended-chain models. Possible derivatives that do not increase the content of the unit cell or change the crystal class are listed in Table 12. Except for the *C2/m* amphiboles, none of the natural amphiboles are adequately described by this type of approach (the natural $P2_1/m$ amphiboles can be thought of as a subgroup derivative of the *C2/m* structure and thus would not have a separate identity within the bounds of this model). Thus the *Pnma* and *Pnmn* cannot be represented by completely rotated (that is, close-packed) models; note that this was also the conclusion of Law & Whittaker (1980) on the basis of arguments concerning close packing.

TABLE 12. EXTENDED CHAIN AND DERIVATIVE ROTATED CHAIN MODELS OF AMPHIBOLES

Extended structure	Rotated structure	O:S ratio	Natural representatives
C2/m	C2/m	all O	C2/m amphiboles
	C2/m	all S	none found
	$P2_1/m$	1:1	none found
Pnmn	$P2_1mn$	1:1	none found
Pnma	$P2_1ma$	3:1	none found
	$P2_1ma$	1:3	none found

modified after Thompson (1970)

Papike & Ross (1970) have examined the structural features of the various amphibole types using this model as the basis of their argument. They also introduced a new feature into the model, emphasizing the "I beam" as an important structural module; the constitution

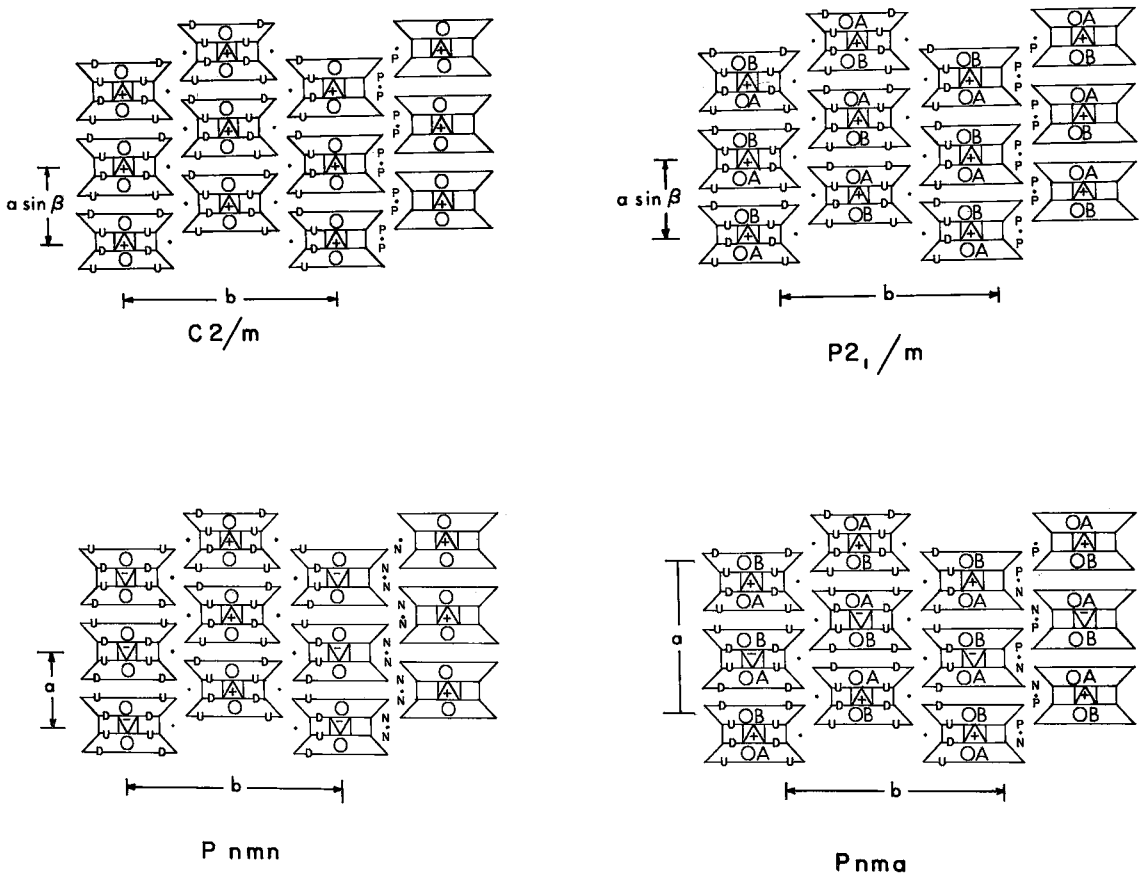

FIG. 22. Ideal I-beam diagrams for the amphibole structures [after Papike & Ross (1970) as modified by Cameron & Papike (1979)]. The diagrams are modified to express the *U.D* nomenclature in terms of the *P.N* symbolism of Sueno *et al.* (1976).

of the I-beam module and its position in a real structure are shown in Figure 9. Thus the rotational aspect of the two double chains in a module is defined with respect to the relative attitude of the constituent octahedra. Geometrical distinctions between the modules give rise to various sheet-stacking sequences along $X\sin\beta$ that account for the various space-groups shown by the principal amphibole structure-types. These stacking sequences are shown in the I-beam diagrams of Figure 22. In relating the completely rotated models to real structures, it is important to be aware of the following constraint: in order for the model to fit together, the sizes of the tetrahedra and octahedra must obey equation (1) of the previous section.

The $C2/m$ structure-type has a beam-stacking sequence (+,+.+,+.) through two unit-cells in the $X\sin\beta$ direction. According to Thompson's parity rule, the tetrahedral double-chains must exhibit the same rotational character in the intercalated tetrahedral layers. Thus a fully rotated $C2/m$ model-structure with this stacking sequence must consist either of all O-rotations or all S-rotations, as this condition is forced by the symmetry in the $C2/m$ model. This is not necessarily the case in subgroups of $C2/m$, and thus in the $P2_1/m$ structure-type with the beam-stacking sequence (+,+.+,+.), alternate tetrahedral layers are symmetrically distinct and mixed rotations are possible. Although this model allows these two monoclinic structure-types to have O- or S-rotations (or both), only O-rotations are observed in refined structures. In fact, all real structures are closer to the extended model, with incomplete O rotations of up to 10° as compared with the value of 30° for completely rotated structures. Perhaps the most significant difference between the $C2/m$ and $P2_1/m$ structure-models of Figure 22 is the existence of two unique tetrahedral double-chains in the latter. This distinction is considerable in the structure of tirodite $P2_1/m$ itself, where the A and B chains show O-rotations of 0.8° and 6.9°, respectively.

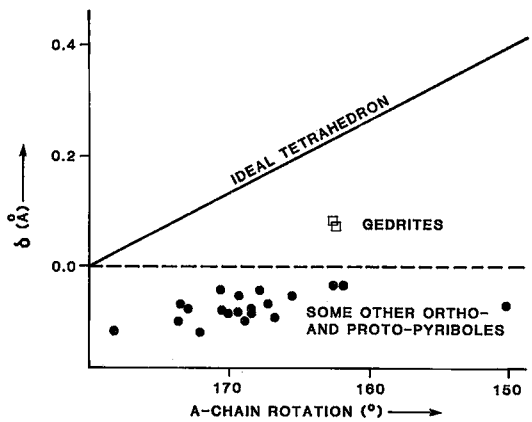

FIG. 23. Misfit parameter δ as a function of chain rotation in the A chain of orthorhombic pyriboles. The diagonal line shows the amount of misfit that would be produced by a chain of regular tetrahedra. The points marked refer to gedrite [32] and [33]. From Veblen & Burnham (1978).

The $P2/a$ structure-type is similar to the $C2/m$ structure-type within the bounds of this model. The beam-stacking sequence is (+,+.+,+.), with symmetrically related alternate tetrahedral layers showing all O-rotations. The loss of the mirror plane compared with the $C2/m$ structure-type affects the internal constitution of the I beams but does not allow any more freedom to their relative arrangement.

The *Pnma* structure-type has a beam-stacking sequence (+,+,−,−.) through one unit cell in the X direction (compare Figs. 16 and 22). There are two symmetrically distinct tetrahedral double-chains that lie on each side of each octahedral strip. The I-beam modules are repeated such that alternate tetrahedral layers are symmetrically distinct. According to the parity rule, alternate tetrahedral layers should show O- and both O- and S-rotations, depending on whether they are sandwiched between (+,+) or (+,−) octahedral layers. As indicated in Figure 22, both *Pnma* and *Pnmn* amphiboles contain only O-rotated chains. The way in which both structures link together while violating the parity rule has been the subject of some discussion, and the utility of the parity rule has been questioned. Papike & Ross (1970) proposed that linkage between layers violating the parity rule occurs by extension of the A chain and distortion of the M2 octahedron. Veblen & Burnham (1978) presented strong evidence to indicate that O rotations (and hence parity violations) in orthopyriboles and protopyriboles are necessitated by stereochemical requirements resulting from polyhedral edge-sharing. Following the argument of Veblen & Burnham (1978), let δ be the difference in z co-ordinates of the O4A and O2A atoms in the A chain of *Pnma* amphiboles. Inspection of the ideal polyhedral models of Figure 21 indicates that δ is a measure of the distortion of the M2 octahedron if linkage is to be maintained (for example, in the lower part of Figure 21, the amount of parity violation indicated by the vertical arrow is seen to

be equal to 2δ); if δ = 0, the ideal polyhedron model fits exactly. Figure 23, from Veblen & Burnham (1978), compares δ values calculated from these ideal pyribole models with the δ values observed in defined pyribole structures. The correspondence is very poor, with the real δ values clustering around zero, and the model even predicting δ values of opposite sign for all pyriboles except gedrite[32] and [33]. Thus in anthophyllite, for example, extension of the A chain will produce increased distortion of the M2 octahedron, in contrast to what would happen in gedrite. The way in which M2 could distort to promote linkage is by extension of the O4A–O4B edge in the *YZ* plane. Comparison of this parameter between the orthorhombic amphiboles (where parity violations occur) and similar *C*2/*m* amphiboles (with no parity violations) should indicate the importance of M2 distortion in this context. The relevant values are: protoamphibole[20] 1.95 Å, anthophyllite[23] 1.92 Å, cummingtonite(21) 1.95 Å; holmquistite[31] 1.75 Å, clinoholmquistite (62) 1.75 Å; gedrite[32] 1.79 Å, gedrite[33] 1.81 Å, no corresponding monoclinic structure. Apart from the gedrites, for which insufficient information is available, this suggests that M2 does not distort significantly because of parity violations in the orthorhombic amphiboles, and supports the view of Veblen & Burnham that the A chain passively adopts the configuration that the octahedral and tetrahedral distortions dictate. This would also accord with the view presented later that the bond-valence requirements of O4A and O4B will, to a large extent, dictate its position. The anomalous position of gedrite in this scheme would appear to stem from the bond-valence requirements of the A-site cation.

The *Pnmn* structure-type has a beam stacking sequence (+,−.+,−.) through two unit cells in the *X* direction. There is only one symmetrically distinct tetrahedral double-chain, and alternate tetrahedral layers are symmetry-related. According to the parity rule, the structure should show equal numbers of O- and S-rotated chains. Of course, this is not compatible with *Pnmn* symmetry, such an arrangement being compatible with a maximum symmetry $P2_1mn$. Following Veblen & Burnham (1978), the violation of the parity rule in protoamphibole is necessitated by the stereochemical requirements of the M2 and T2 polyhedra.

Using the nomenclature of this model, the principal amphibole structure-types can be summarized as follows: (i) *C*2/*m*: stacking sequence (+,+.+,+.), all O-rotations, (ii) $P2_1/m$: stacking sequence (+,+.+,+.), all O-rotations with alternate symmetrically distinct tetrahedral layers, (iii) *P*2/*a*: stacking sequence (+,+.+,+.), all O-rotations, (iv) *Pnma*: stacking sequence (+,+,−,−.), all O-rotations with alternate symmetrically distinct tetrahedral layers, and (v) *Pnmn*: stacking sequence (+,−.+,−.), all O-rotations.

Veblen & Burnham (1978) questioned the utility of pyribole models based on holosymmetric polyhedra, particularly with regard to the notion of parity. Based on the fact that the parity rule predicts structural misfit associated with pyribole A chains, and the

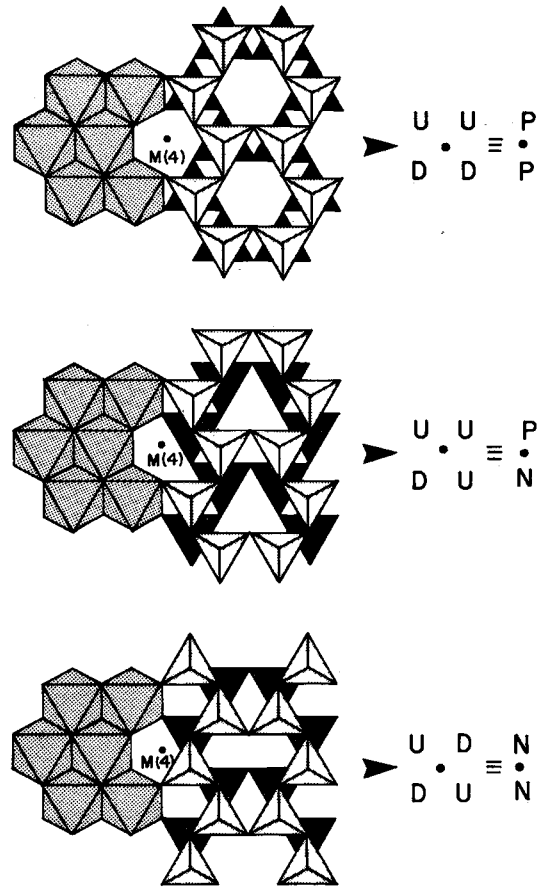

FIG. 24. Tetrahedral chain configurations around the M(4) site for ideal, completely rotated structures, projected down [100]; modified after Cameron & Papike (1979) according to the nomenclature introduced by Sueno *et al.* (1976) for the pyroxenes.

TABLE 13. EQUIVALENCE RELATIONSHIPS BETWEEN STACKING SYMBOLS*

U	D	D	U	N											
D	U	U	D	N											
D	D	U	D	D	U	U	U	P	N						
U	D	D	D	U	U	D	U	N	P						
U	U	D	D	P											
D	D	U	U	P											

*from Cameron & Papike (1979) and Sueno et al. (1976)

sign of the misfit is generally wrong, this suggests that the concept of parity is not useful and could be discarded.

In a discussion of pyroxene geometry, Papike *et al.* (1973) introduced a modification to the I-beam diagram that clarifies the polyhedral relationships surrounding the M2 site. Subsequently, Cameron & Papike (1979) have examined the amphibole structures using this approach. The idea of O- and S-rotations has been used to examine the linkage possibilities in the *X* direction. However, intermodule linkage also occurs in the *Y* direction, and several distinct arrangements exist. As these result in differing arrangements of tetrahedra in the vicinity of the M(4) site, this approach is of particular interest owing to the importance of the M(4) site in phase relations of amphiboles (Warren 1930, Whittaker 1960, Papike *et al.* 1969). The nomenclature is based on the relative orientations of the triangular faces that are parallel to (100) and belong to the octahedra and tetrahedra that link together in the *Y* direction. Triangular faces that point in the $-Z$ direction are referred to as D (down). The possible distinct arrangements are illustrated in Figure 24, accompanied by the representative nomenclature. The solid dot represents the M(4) site when viewed along the $-Z$ direction, with the surrounding letters representing the orientation of the triangular faces of the M(1) octahedron (left-hand column) and the tetrahedra (right-hand column). Equivalence relationships between all possible configurations are shown in Table 13.

A simpler notation was introduced with regard to the pyroxenes by Sueno *et al.* (1976). Here, an N (negative) configuration occurs where the basal triangular faces of the tetrahedral chain point in the opposite direction to the parallel triangular faces of the octahedra (M1 in the pyroxenes) to which they link in the *Y* direction. A P (positive) configuration occurs where the triangular faces of the tetrahedral chain point in the same direction as the parallel triangular faces of the octahedra to which they link in the *Y* direction. As with the previous nomenclature, the solid dot represents the M(4) site as viewed along the $-Z$ direction, with the relevant letters above and below. The relation between this and the previous nomenclature is shown in Table 13 and in Figures 22 and 24. In the completely rotated ideal structures, only combinations of O with P (U.U or D.D) and S with N (U.D or D.U) occur if close packing is to be preserved (Sueno *et al.* 1976). As is evident in Figure 22, this is not the case in the *Pnma* and *Pnmn* amphiboles, where O–N combinations occur as a result of distortions in the real structures.

A more general model has recently been introduced by Chisholm (1981). This is also based on the I-beam model, but allows partially rotated chains and some tetrahedral distortion to occur; consequently the model is not bound by the parity rule of Thompson (1970). With the constraint that a structure may contain two types of tetrahedral layers but that each layer must contain only one type of tetrahedral chain, a set of model pyribole structures can be derived that includes all of the known amphibole structure-types.

A close-packing approach

Law & Whittaker (1980) have considered rotated-chain models of amphiboles from the viewpoint of close-packed structures. There are four close-packed layers of oxygen atoms in a I-beam unit. Using standard nomenclature (Wells 1962), there are a total of 24 arrangements of the A, B and C layers; not all of these arrangements are unique. Using the operations of cyclic permutation (A→B, B→C, C→A) and sequence reversal, it can be shown that there are only three fundamental types of sequence: (i) first and last symbols identical, inner two different: ABCA; (ii) first and third symbols identical, second and fourth identical: ABAB; and (iii) first and third symbols identical, second and fourth different: *ABAC*.

The tetrahedral cations occupy sites between layers 1 and 2 and between layers 3 and 4, and have the same arrangement as the oxygen atoms of layers 2 and 3 to which they are bonded. The octahedral cations occupy sites

between layers 2 and 3 in an arrangement that differs from both these layers. If the cation arrangements are denoted by lower-case letters, the full I-beam structure can be symbolized. As the tetrahedral cation array is identical with the corresponding inner oxygen array, there is no loss of information on omitting its symbol; hence *AbBaCcB* contracts to *ABaCB*. The presence of three upper-case symbols indicates cubic close-packing (O rotation), and the presence of two upper-case symbols indicates hexagonal close-packing (S rotation). Law & Whittaker (1980) defined the cyclic sequence $A \rightarrow B \rightarrow C \rightarrow A$ as being accompanied by a shift of one-third of the projected inter-oxygen distance ($c/6$ for amphiboles) along the negative direction of the Z axis of amphibole. Thus octahedra are positively directed if the two layer symbols involved are in cyclic order (*AB, BC, CA*) reading upward and negatively directed if the order is reversed (*BA, CB, AC*). The definition of octahedron direction is actually arbitrary, as it depends on the choice of the direction of the Z axis and on the decision as to which arrays are denoted *A, B* and *C*. The complete list of I beams (equivalents included) is shown in Table 14 together with the equivalent O/S rotation symbol. Ignoring orientation both along Z and orthogonal to the layers, there are only three basic I-beam types: [O±O], [O±S] and [S±S], corresponding to the three types of stacking sequence.

There is only one way in which fully rotated tetrahedral chains can be placed side-by-side such that the constituent oxygen atoms lie on a pair of coherent close-packed arrays (Fig. 25); any other arrangement would lead to a discontinuity in an oxygen layer. In terms of the oxygen stacking-sequence, if the I-beam symbols are written on one line, then the same symbols written on the next line but divided up differently correspond to the adjacent stack of I beams. A limit on the possible number of structures generated by stacking variations may be imposed by requiring the stacking sequence to repeat every four or eight layers (corresponding to real amphibole structures). The five types of structure possible for a four-layer repeat are shown in Table 15. In each I-beam stack, the first symbol of the second I-beam must differ from the last symbol of the first, so that for each of the three types of

TABLE 14. COMPLETE LIST OF I BEAMS IN THE A/B/C AND O/S NOTATIONS. ALL SYMBOLS ON ONE LINE ARE EQUIVALENT

ABcAB	BCaBC	CAbCA	[S-S]
ABcAC	BCaBA	CAbCB	[S-O]
ABaCA	BCbAB	CAcBC	[O+O]
ABaCB	BCbAC	CAcBA	[O+S]
ACbAB	BAcBC	CBaCA	[S+O]
ACbAC	BAcBA	CBaCB	[S+S]
ACaBA	BAbCB	CBcAC	[O-O]
ACaBC	BAbCA	CBcAB	[O-S]

from Law & Whittaker (1980)

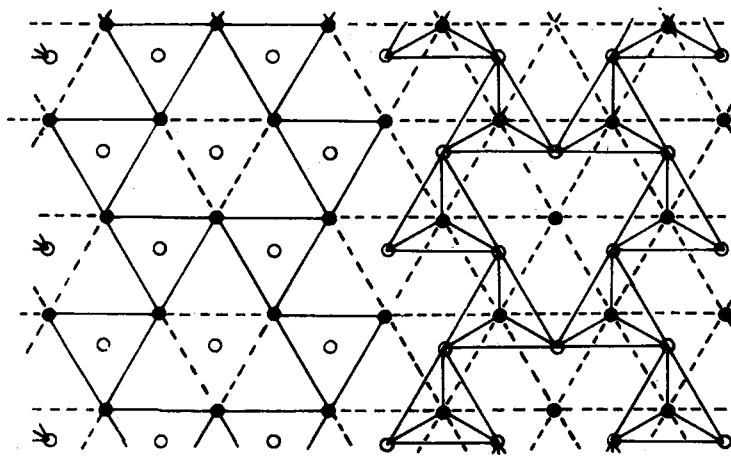

FIG. 25. Side-by-side stacking of fully rotated tetrahedral chains showing how continuous octahedral layers are formed [from Law & Whittaker (1980)].

TABLE 15. THE FIVE POSSIBLE STRUCTURES FOR A FOUR-LAYER REPEAT IN BOTH A/B/C AND O/S SYMBOLS

1.	.ABaCA.BCbAB.CAcBC.ABaCA. ...=	.0+0.0+0.0+0.0+0.
	bAB.CAcBC.ABaCA.BCbAB.CAc ...=	+0.0+0.0+0.0+0.0+
2.	.ABcAB.ABcAB.ABcAB.ABcAB. ...=	.S-S.S-S.S-S.S-S.
	cAB.ABcAB.ABcAB.ABcAB.ABc ...=	-S.S-S.S-S.S-S.S-
3.	.ABaCB.ABaCB.ABaCB.ABaCB. ...=	.0+S.0+S.0+S.0+S.
	cAB.CBcAB.CBcAB.CBcAB.CBc ...=	-S.0-S.0-S.0-S.0-
4.	.ABcAC.BCaBA.CAbCB.ABcAC. ...=	.S-0.S-0.S-0.S-0.
	cAB.ACaBC.BAbCA.CBcAB.ACa ...=	-S.0-S.0-S.0-S.0-
5.	.ABaCA.CAcBC.BCbAB.ABaCA. ...=	0+0.0+0.0+0.0+0
	cAB.CAbCA.BCaBC.ABcAB.CAb ...=	S.S-S.S-S.S-S.S

from Law & Whittaker (1980)

I beam ([O±O], [O±S] and [S±S]), there are two possibilities. Structure-type 5 combines two of these possibilities, and hence there are a total of five structures possible.

When considering structures in which I beams within a stack differ in type or orientation, Law & Whittaker (1980) introduced an alternative notation of stacking. Lower-case letters are used to designate oxygen-atom layers where local arrangement is of hexagonal (h) or cubic (c) type according to whether its neighbors in adjacent layers lie on the same array as each other or lie on different arrays. Layers linked by strips of octahedral cations are separated by '.', corresponding to both '.' and the lower-case letter in the *A,B,C* notation. The relationship between the two notations is shown in Table 16. Law & Whittaker (1980) indicated that there are twenty-two sequences that repeat in eight layers with two I-beams; these are also shown in Table 16 together with the corresponding *A,B,C* and *O,S* designations.

TABLE 16. STACKING SEQUENCES FOR AMPHIBOLES

Stacking sequence	A,B,C notation (first stack)	I-beam types 1st stack	2nd stack	β	Space group
Sequences repeating in four layers					
hh.hh.hh.hh.	AB.AB.(rep)	*S-S.S-S.	S-S.S-S.	90°	C2/m
hh.cc.hh.cc.	AB.AC.($B^{\sim}$)	*S-0.S-0.	0-S.0-S.	109.47°	$P2_1/m$
hc.hc.hc.hc.	AB.CB.(rep)	*0+S.0+S.	0-S.0-S.	ortho	$P2_1mn$
hc.ch.hc.ch.	AB.CA.($C^{\sim}$)	0+0.0+0.	S-S.S-S.	100.02°	P2/m
cc.cc.cc.cc.	AB.CA.($B^{\sim}$)	*0+0.0+0.	0+0.0+0.	109.47°	C2/m
sequences repeating in eight layers					
hh.hh.hh.cc.	AB.AB.AB.AC.($B^{\sim}$)	S-S.S-0.	S-S.0-S.	100.02°	$P2_1/m$
hh.hh.hc.hc.	AB.AB.AB.CB.(rep)	S-S.0+S.	S-S.0-S.	90°	Pm
hh.hh.ch.hc.	AB.AB.AC.AC.($B^{\sim}$)	S-S.S+S.	S-0.0-S.	100.02°	P2/m
hh.hh.hc.ch.	AB.AB.AB.CA.($C^{\sim}$)	S-S.0+0.	S-S.S-S.	95.05°	P2/m
hh.hh.cc.cc.	AB.AB.AC.BA.($C^{\sim}$)	S-S.0-0.	S-0.0-S.	95.05°	P2/m
hh.hc.hh.hc.	AB.AB.CB.CB.(rep)	S-S.S+S.	0+S.0-S.	ortho	$P2_1ma$
hh.hc.hh.ch.	AB.AB.CB.CA.($C^{\sim}$)	S-S.S+0.	0+S.S-S.	95.05°	$P2_1/m$
hh.hc.hc.cc.	AB.AB.CB.AC.($B^{\sim}$)	S-S.0-0.	0+S.0-S.	100.02°	Pm^1
hh.hc.ch.cc.	AB.AB.CA.CB.(rep)	S-S.S-0.	0+0.0-S.	90°	Pm
hh.hc.cc.hc.	AB.AB.CA.BA.($C^{\sim}$)	S-S.0+S.	0+0.0-S.	95.05°	Pm
hh.hc.cc.ch.	AB.AB.CA.BC.($B^{\sim}$)	S-S.0+0.	0+0.S-S.	100.02°	$P2_1/m$
hh.ch.hc.cc.	AB.AC.AC.BA.($C^{\sim}$)	S-0.0-0.	S+S.0-S.	95.05°	Pm^1
hh.ch.ch.cc.	AB.AC.AB.AC.($B^{\sim}$)	*S-0.S-0.	S+0.0-S.	100.02°	Pm
hh.ch.cc.hc.	AB.AC.AB.CB.(rep)	*S-0.0+S.	S+0.0-S.	90°	$P2_1/m$
hh.cc.cc.cc.	AB.AC.BA.CB.(rep)	S-0.0-0.	0-0.0-S.	90°	$P2_1/m$
hc.hc.hc.ch.	AB.CB.AB.CA.($C^{\sim}$)	0+S.0+0.	0-S.S-S.	95.05°	Pm^1
hc.hc.ch.ch.	AB.CB.AC.AB.(rep)	0+S.S+0.	0-S.S-S.	90°	P2/m
hc.hc.cc.cc.	AB.CB.AC.BA.($C^{\sim}$)	0+S.0-0.	0-0.0-S.	95.05°	Pm
hc.ch.cc.cc.	AB.CA.CB.AC.($B^{\sim}$)	0+0.0-0.	S-0.0-S.	100.02°	P2/m
hc.cc.hc.cc.	AB.CA.BA.CB.(rep)	0+0.0-0.	0+S.0-S.	ortho	$P2_1ma$
hc.cc.ch.cc.	AB.CA.BC.BA.($C^{\sim}$)	0+0.S-0.	0+0.0-S.	95.05°	Pm^1
hc.cc.cc.ch.	AB.CA.BC.AB.(rep)	0+0.0+0.	0+0.S-S.	90°	Pm

Notes: In the second column, (rep) indicates that the next I-beam in the sequence is the same as the first; ($B^{\sim}$) or ($C^{\sim}$) indicates that it begins with B or C and repeats by one or by two cyclic permutations respectively. In the third column sequences which contain only one type of I-beam (i.e. all [O±O], all[S±S], or all [O±S] or [S±O] are starred.

It is interesting to examine the orthoamphibole structures using this symbolism. Papike & Ross (1970) gave the I-beam sequence as +,+,−,− in the *Pnma* amphibole structure; note that alternate symbols relate to I beams in adjacent stacks (Fig. 22). The corresponding sequence is thus:

.0+0.0–0. or ABaCA.BAbCB.ABaCA
+0.0–0.0+ or AB.ACaBA.BCbAB.AC

with an eight-layer repeat. This shows that alternate pairs of oxygen layers would not match up as continuous close-packed layers across the two stacks, and hence the *Pnma* amphibole structure cannot be related to the fully rotated model. For protoamphibole, the I-beam sequence was given +,−,+,−. The corresponding sequence in the current nomenclature is:

.0+0.0+0. or ABaCA.ABaCA.ABaCA
–0.0–0.0– or BA.ACaBA.ACaBA.AC

As indicated by Law & Whittaker (1980), this cannot correspond to a close-packed stacking, as a single stack contains identical symbols adjacent to one another. Thus, the *Pnmn* amphibole structure cannot be related to the fully rotated (close-packed) models.

Polysomatic structures

Thompson (1970, 1978) has suggested that amphiboles be regarded as layers of trioctahedral mica and pyroxene, alternating along the amphibole *Y* axis. An amphibole I-beam (Fig. 26) can be factored into a central mica part and two flanking pyroxene parts. If the amphibole structure is considered as an assemblage of I beams, such a factorization results in alternating layer modules of mica and pyroxene (Fig. 26). Removal of the mica layers from a *C2/m* amphibole, together with a relative translation of (*b*/4 plus *c*/2) for adjacent pyroxene layers results in an idealized *C2/c* pyroxene. Similarly, removal of the pyroxene layers and relative translation of adjacent mica layers by (*b*/4 plus *c*/2 plus *a*/2) result in an idealized 1M talc, space group *C2/m*. The idealized protoamphibole (*Pnmn*) structure can be regarded as alternating layers of protoenstatite and 1M talc (with the talc in adjacent M slabs in different orientations). The idealized anthophyllite (*Pnma*) structure can be regarded as alternating layers of orthoenstatite and a 2O talc.

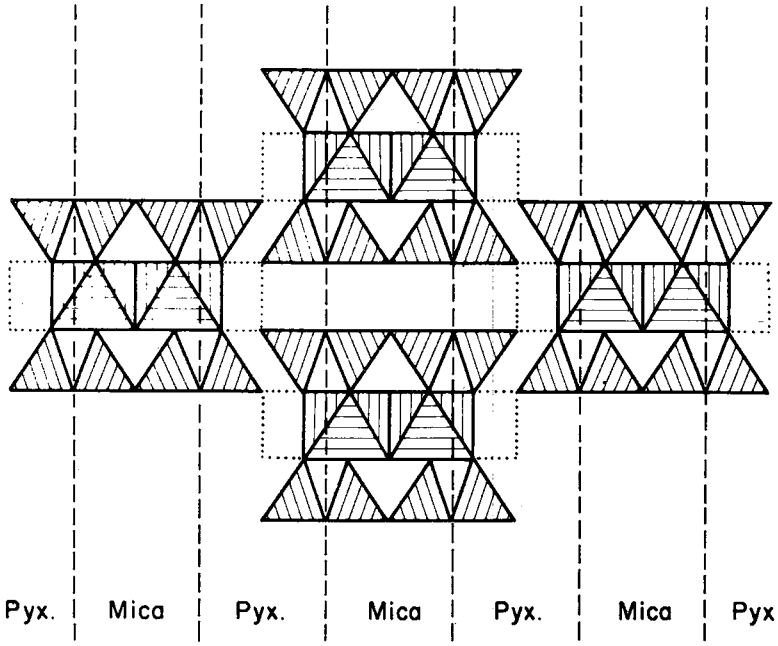

FIG. 26. I-beam diagram of a $C2/m$ amphibole projected down Z; the broken vertical lines show the (010) cuts that factor it into pyroxene and mica layers [from Thompson (1978)].

Thompson (1978) introduced the terms *polysome* to designate a crystal that can be regarded as made of chemically distinct layer-modules, and *polysomatic series* to designate a series of minerals that can be regarded as being made up from the same basic set of modules. Writing mica schematically as (M) and pyroxene as (P), we may write amphibole as (MP); examples of series involving these three polysomes are given in Table 17. Such relationships may simplify chemographic analysis of natural assemblages. More complex intermediate polysomes have been found [(MMP) and (MPMMP): Veblen & Burnham (1975, 1976)], giving further justification to the idea of polysomatic series.

TABLE 17. POLYSOMATIC SERIES IN THE BIOPYRIBOLES

Talc	+	Diopside	=	Tremolite
$Mg_3Si_4O_{10}(OH)_2$		$Ca_2Mg_2Si_4O_{12}$		$Ca_2Mg_5Si_8O_{22}(OH)_2$
Talc	+	Enstatite	=	Anthophyllite
$Mg_3Si_4O_{10}(OH)_2$		$Mg_4Si_4O_{12}$		$Mg_7Si_8O_{22}(OH)_2$
Talc	+	Jadeite	=	Glaucophane
$Mg_3Si_4O_{10}(OH)_2$		$Na_2Al_2Si_4O_{12}$		$Na_2Mg_3Al_2Si_8O_{22}(OH)_2$
(Fe-Talc)*	+	Acmite	=	Riebeckite
$Fe_3Si_4O_{10}(OH)_2$		$Na_2Fe_2Si_4O_{12}$		$Na_2Fe_5Si_8O_{22}(OH)_2$
Phlogopite	+	Diopside	=	(K-Edenite)*
$KMg_3AlSi_3O_{10}(OH)_2$		$Ca_2Mg_2Si_4O_{12}$		$KCa_2Mg_5AlSi_7O_{22}(OH)_2$
Na-Phlogopite	+	Diopside	=	Edenite
$NaMg_3AlSi_3O_{10}(OH)_2$		$Ca_2Mg_2Si_4O_{12}$		$NaCa_2Mg_5AlSi_7O_{22}(OH)_2$
Talc	+	"CATS"	=	Tschermakite
$Mg_3Si_4O_{10}(OH)_2$		$Ca_2Al_4Si_2O_{12}$		$Ca_2Mg_3Al_4Si_6O_{22}(OH)_2$

*minerals in parentheses have not been found.
From Thompson (1978).

Crystallographic shear-structures

A crystallographic shear-plane (CS plane) is an extended planar defect that occurs in a series of structures with the same packing arrangement of anions. It is defined by the indices and position of the plane and the displacement vector, a component of which must be orthogonal to the plane. At the CS plane, the linkage of cation polyhedra is altered, resulting in a local change in chemical composition and the possible generation of new co-ordination polyhedra into which additional cations may be incorporated. It is important to stress that the anion packing is not affected by the presence of the CS plane.

The idea of pyroxenes, amphiboles and micas as a family of shear structures was proposed

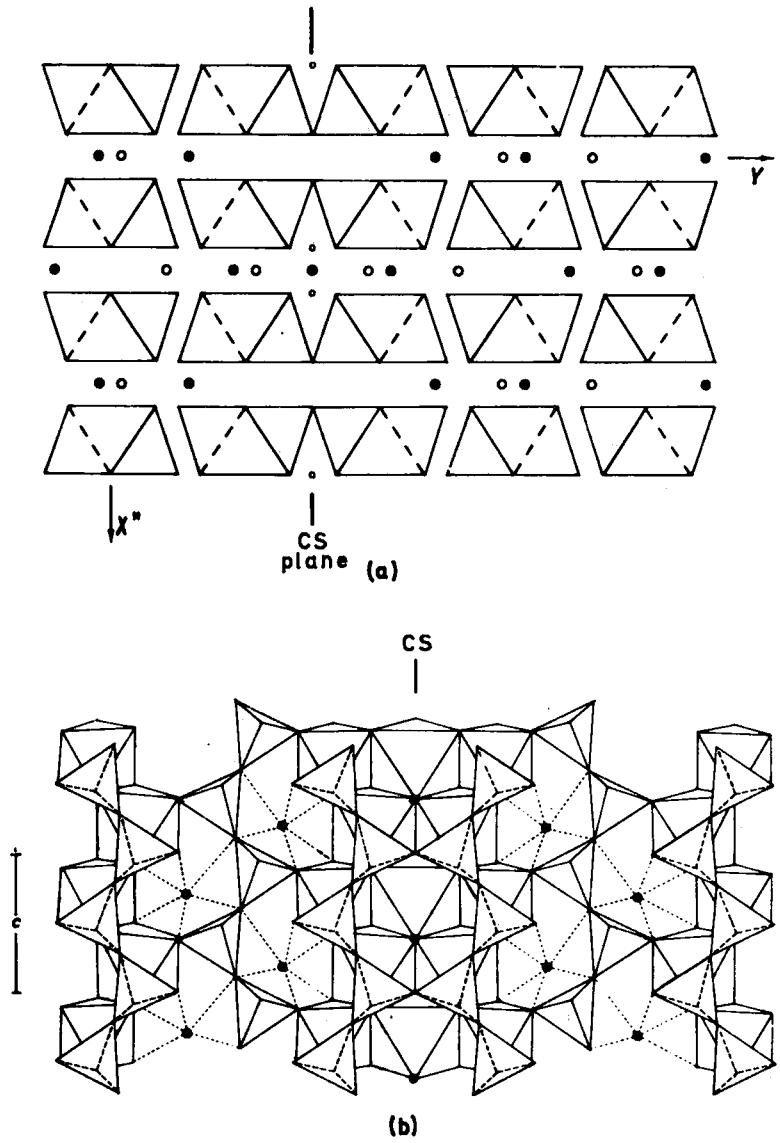

FIG. 27. Schematic diagram of an (010) crystallographic shear (CS) plane in pyroxene viewed down Z (top) and down [100] (bottom). Note the formation of amphibole-like structure within the pyroxene by this method [from Chisholm (1975)].

by Chisholm (1973) and further developed by Chisholm (1975). Pyroxene is the basic structure. Consider a planar fault //(010) with a displacement vector ½(**b**+**c**) or ½(**c**+**a**); these vectors are equivalent in $C2/c$ and very similar in $P2_1/c$. Displacement plus minor compositional changes to maintain electroneutrality result in the generation of an amphibole-like region within the pyroxene (Fig. 27). A regular superstructure of these CS planes every second chain corresponds to the amphibole structural arrangement (Fig. 28), whereas occurrence of these CS planes every chain generates a talc or mica structure (Fig. 29).

This formulation is similar but not equivalent to the polysomatic series formulation of

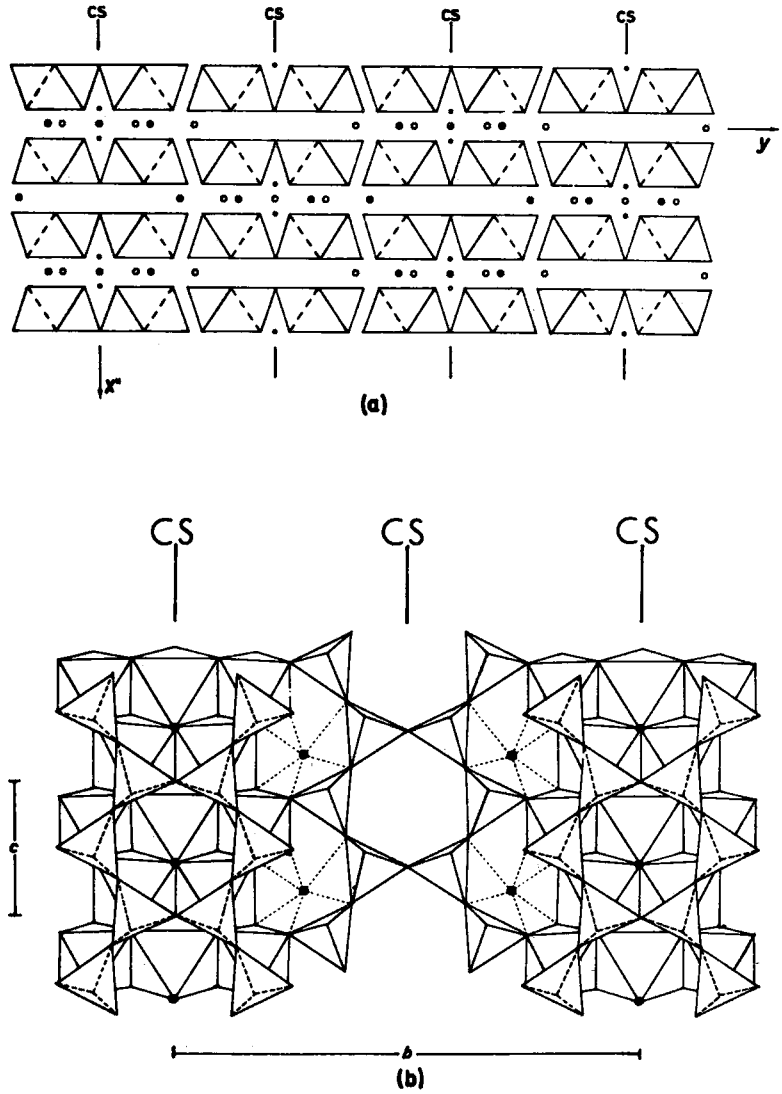

FIG. 28. Schematic diagram of the amphibole structure down Z (top) and down [100] (bottom); note the (010) CS plane every second chain [from Chisholm (1975)].

Thompson (1978). The mica module of Thompson (1978) is centred on the CS plane of Chisholm (1975); the local compositional change in a pyroxene with one CS plane of the type indicated above corresponds either to a ribbon of talc (corresponding to one mica module) or to a ribbon of amphibole (corresponding to one mica module flanked by two pyroxene modules), depending on the width of the region considered. In the shear-structure formulation, an ordered but unequally spaced arrangement of CS planes can give rise to the wider chain pyriboles (*cf.* Veblen & Burnham 1978); the microstructures that have recently been found in biopyriboles (Veblen & Buseck 1979, 1980) can be described in terms of Wadsley defects.

Although similar in aspect, the polysomatic and CS formulations were developed with different applications in mind, and it is here that the conceptual differences become apparent. The polysomatic model was developed primarily to amplify and simplify chemographic relationships among these phases in composition space (Thompson 1978); it can perhaps be

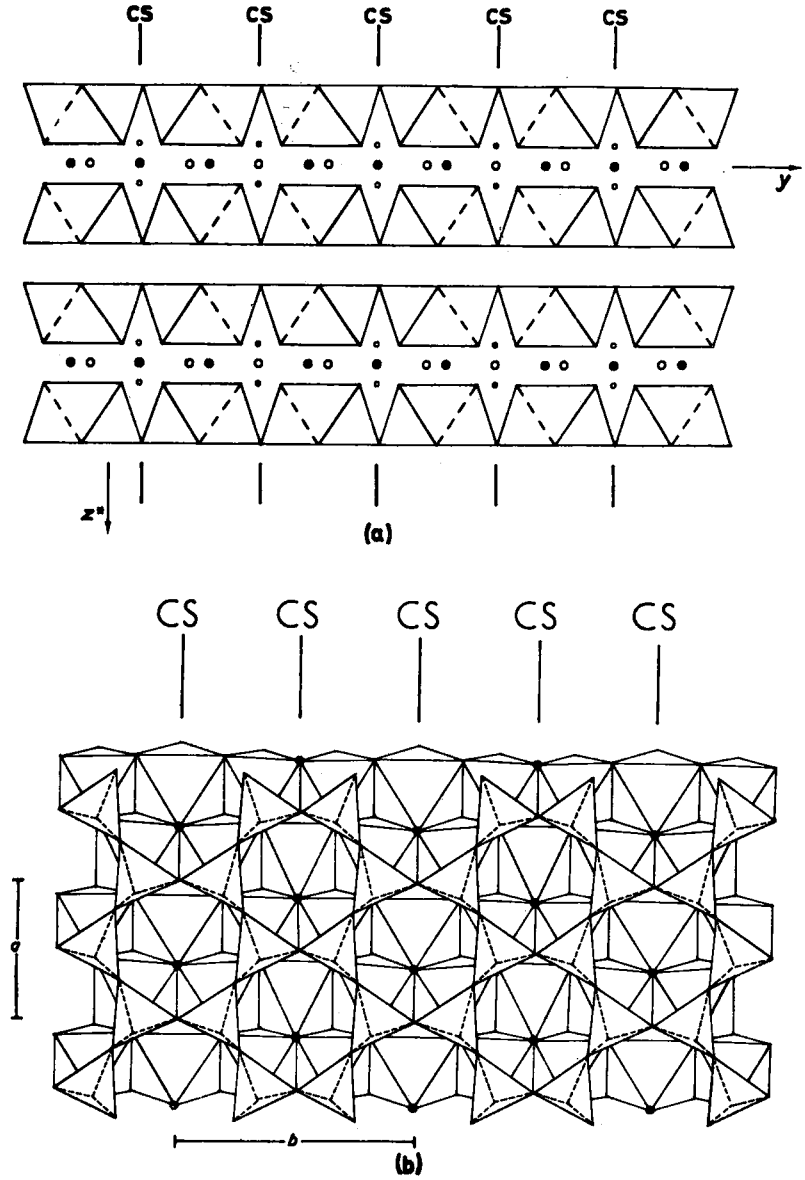

FIG. 29. Schematic diagram of the talc structure viewed down X (top) and down [001] (bottom); note the presence of an (010) CS plane at every chain [from Chisholm (1975)].

described as a structural model with chemical implications. An additional feature of the polysomatic model is that it can be used to predict atomic positions in biopyriboles quite accurately, whereas the CS model cannot (David Veblen, pers. comm.). The CS model was developed primarily to interpret the reaction mechanisms between these phases (Chisholm 1975); it can perhaps be described as a structural model with kinetic implications. However, the real reaction mechanisms as observed in HRTEM experiments do not involve CS planes (Veblen & Buseck 1979, 1980), and hence the CS model is of questionable utility.

Some remarks on model structures

It is the author's opinion that the proliferation of model structures in the biopyriboles has got completely out of hand. Numerous different formulations exist, and the complexity of this topic far exceeds the complexity of the natural structures. Model building should be a pragmatic occupation; if it's not useful, don't do it.

The Tetrahedral Double Chain in Non-^{iv}Al Amphiboles

There are considerable stereochemical variations in the tetrahedral double-chain from structure to structure. This is presumably in response to the differing local environments and has led to examination of the double-chain element in terms of various models of bonding.

From a molecular orbital viewpoint, several predictions can be made concerning the stereochemistry of polymerized tetrahedra (Brown *et al.* 1969, Gibbs *et al.* 1972): (i) Si–O(nbr) bonds are usually shorter than Si–O(br) bonds, providing the Si–O(br)–Si angle is not wide and $\overline{\chi}$ (the mean electronegativity of the nontetrahedral cations) is not large; (ii) the shorter Si–O(br) bonds are usually associated with the wider Si–O(br)–Si angles, with Si–O(br) an inverse function of cos(Si–O(br)–Si); (iii) tetrahedral angles usually decrease in the order O(nbr)–Si–O(nbr) > O(nbr)–Si–O(br) > O(br)–Si–O(br), and (iv) Si–O bond lengths are a function of the O–Si–O angles in which they are involved. These predictions provide a framework within which the variations in tetrahedral stereochemistry may be examined.

Bond-valence models are related to the fact that deviations from Pauling's second rule (Pauling 1929, 1960) are correlated with variations in cation-anion distances in structures. Several schemes that relate bond lengths to bond valences have been developed; of these, the treatments of Baur (1970, 1971) and Brown & Shannon (1973) are the more general. Baur (1971) has derived an equation relating Si–O bond length to the deviation from the mean bond-strength sum of all anions co-ordinating a specific Si exhibited by a specific anion. This equation may be used both to predict individual bond-lengths absolutely from a forecast mean bond-length, or it may be used in conjunction with the observed mean bond-length to predict deviations from that mean. Brown & Shannon (1973) have derived curves relating bond length to bond valence. Although the curves are not immediately predictive as is the scheme of Bauer (1970, 1971), they recognize weak bonding interactions that are either ignored or overemphasized in the previous method. Additional bond-valence curves, including some for the F anion, have been presented by Brown & Wu (1976) and Brown (1978). Both these methods are of considerable use in the interpretation of the detailed stereochemistry of the amphiboles.

The C2/m amphiboles

There are two unique cation-sites with pseudo-tetrahedral co-ordination in this structure type, the T(1) and T(2) sites. Figure 11 shows the details of their co-ordination. Both sites have point-symmetry 1 and are surrounded by four oxygen anions. The T(1) tetrahedron shares one corner with an adjacent T(1) tetrahedron, one corner with an adjacent T(2) tetrahedron, one corner with the other adjacent T(2) tetrahedron and with a [6]-co-ordinate M(4) polyhedron, and the fourth corner with the M(1), M(2) and M(3) octahedra; in addition, it shares one edge with an [8]-co-ordinate M(4) polyhedron. The T(2) tetrahedron shares one corner with an adjacent T(1) tetrahedron, one corner with the other adjacent T(1) tetrahedron and with an [8]-co-ordinate M(4) polyhedron, one corner with the M(2) octahedron and a fourth corner with the M(1), M(2) and M(4) polyhedra; in addition, it shares one edge with the M(4) polyhedron.

Brown & Gibbs (1969, 1970) examined the steric details in the double chains of four $C2/m$ amphiboles and showed that they conform to the predictions of the molecular orbital model; in addition, they correlated individual Si–O bond lengths with $\overline{\chi}$ (the mean electronegativity of the nontetrahedral cations). This approach was developed further by Mitchell *et al.* (1971), who presented equations relating the T–O(nbr) bond lengths to <T–O(br)–T> and $\overline{\chi}$:

$$\text{T(1)–O(1)} = 1.137 + 0.0029\langle\text{T–O(5, 6, 7)–T}\rangle + 0.051\overline{\chi}_{\text{O(1)}}$$

$$\text{T(2)–O(2)} = 1.211 + 0.0029\langle\text{T–O(5, 6)–T}\rangle + 0.007\overline{\chi}_{\text{O(2)}}$$

$$\text{T(2)–O(4)} = 1.213 + 0.0026\langle\text{T–O(5, 6)–T}\rangle + 0.009\overline{\chi}_{\text{O(4)}}$$

A comparison of the bond lengths calculated from these equations with the observed values for the $C2/m$ amphiboles is given in Figure 30. Mitchell *et al.* (1971) also showed that the T(2)–O(br) distances vary inversely with both T(2)–O(2) and T(2)–O(4). Assuming that the average bond-order of an Si–O bond in an SiO_4 tetrahedron is 1.5 and using the equation